Laser-based micro-sintering of 3D direct laser-written optomechanical resonators

Johanna Sophia Stein

Bachelorarbeit in Physik
angefertigt im Physikalischen Institut

vorgelegt der
Mathematisch-Naturwissenschaftlichen Fakultät
der
Rheinischen Friedrich-Wilhelms-Universität
Bonn

Januar 2025

Ich versichere, dass ich diese Arbeit selbstständig verfasst und keine anderen als die angegebenen Quellen und Hilfsmittel benutzt sowie die Zitate kenntlich gemacht habe.

Bonn, 29.01.2025
Datum

J. Stein
Unterschrift

1. Gutachter: Prof. Dr. Hofferberth
2. Gutachter: Prof. Dr. Linden

Acknowledgements

For welcoming and integrating me so lovely in the group I would like to thank everybody of the Nonlinear Quantum Optics group.
Moreover I would like to thank Prof. Dr. Hofferberth for giving me the opportunity to work on such an interesting project and Prof. Dr. Linden for letting me use the Nanoscribe and for being my second appraiser.
Especially I want to thank Lukas, Florian, Daniel, Benedikt, Jana and Hannes from the FCO for guiding me and making the office a great place to be around and Paul from the Linden group for helping me whenever there were problems at the shooting setup.
Furthermore I would like to thank Nina Heinze, Lukas, Florian and Hannes for the proof reading of this thesis.
Special thanks to my family for supporting and motivating me.

Contents

CHAPTER 1

Introduction

Cavity optomechanics started to attract attention during the development of the principles and technologies of the mechanical measurements of gravitational wave detectors based on interferometry [1]. This research field deals with the radiation-pressure of individual photons in repeated light circulation [2]. Through this radiation-pressure macroscopic mechanical objects and degrees of freedom of an optical system can couple to each other. If this coupling in an optomechanical system is strong enough, quantum effects are occurring [3]. In order to reach the quantum regime with optomechanical coupling Thompson et al. [3] firstly used a semi-transparent micro-mechanical oscillator inside an optical Fabry-Perot cavity as the mechanical element in an cavity optomechanical experiment. Such a system is known as "Membrane-In-the-Middle" (MIM). A MIM system is also used in the Fiber-Cavity-Optomechanics (FCO) experiment of the Nonlinear-Quantum-Optics (NQO) group. In the optomechanical experiment 3D direct laser-written polymer membranes are used inside of fiber Fabry-Perot cavities [4]. 3D direct laser-writing (DLW) enables to fabricate largely unconstrained shapes of mechanical resonators as well as multi-element structures. For the 3D DLW, where liquid resin is polymerised by a focused laser beam, the Nanoscribe PPGT+ (Photonic Professional GT+) is used, shown in picture 2.2.
The objective is dipped into the liquid resin and a pulsed femtosecond fiber laser with the centre wavelength at 780 nm [5] causes polymerisation of the resin. The polymerisation of 2PP (two photon polymerisation) negative-tone resins is induced by free radical polymerisation, where polymer chains are formed through a chemical reaction induced by the energy of the laser beam [6]. To be able to print features on a sub-micrometer scale a non-linear two-photon absorption process (further information in [7]) is used which leads to the production of voxels. With multiple of those voxels whole structures can be printed by moving the focal spot of the laser along trajectories in all three dimensions [7] (see picture 2.3). There are two ways to do this. The first way is the piezo printing mode, where the trajectories are achieved by the piezo-stage, that can move the substrate relative to the laser focus in all three dimensions. The second way is the galvo printing mode, where the trajectories are achieved through two rotatable galvo mirrors, that can move the laser focus in the x-y-plane and the z-axis is adjustable by the piezo-stage [8].
In the experiment a high mechanical quality factor (Q-factor) is important for reaching the quantum regime [9]. Since this Q-factor is limited by the material properties of the polymer resin [9], in this thesis a new method to fabricate silica-based membranes using direct laser-writing is developed. The Q-factor of the current used membranes in the experiment is about $Q \approx 20$ [9]. With other materials of the membranes such as fused silica the Q-factor can be increased to $Q > 1000$ [10]. For that the resin

GP-Silica, which contains nano particles of fused silica, is used. In its normal fabrication process a sintering step after the DLW-printing turns the printed structure into glass. In this sintering step the structure is heated up to 1 300 °C [11]. As we fabricate the mechanical resonators in DLW directly on mirrors from dielectric Bragg reflectors, which can't withstand such temperatures, it is explored, if it is possible using localised laser-based micro-sintering instead.
The structure of this thesis is as follows. In chapter 2 the resin GP-Silica is introduced. The printing process with GP-Silica and the procedure of finding working printing parameters for membranes is explained in chapter 3. In chapter 4 it is then verified, if laser-based micro-sintering can be used instead of an oven for turning the membranes into glass and it is looked for shooting parameters. In the last chapter 5 the coupling map scans of the membranes are done.

CHAPTER 2

GP-Silica

GP-Silica is used for the fabrication of the desired optomechanical resonators (membranes) out of glass. GP-Silica is a highly viscous liquid negative-tone 2PP photo-resin designed for 3D microfabrication of fused silica glass by Nanoscribe[1] [12]. The resin contains nano particles of fused silica. In an e-mail conversation with the Nanoscribe Support they pointed out that the glass particle sizes are below 100 nm and the concentration is below 40% volumetric. The fabrication process this resin is designed for is shown in picture 2.1.

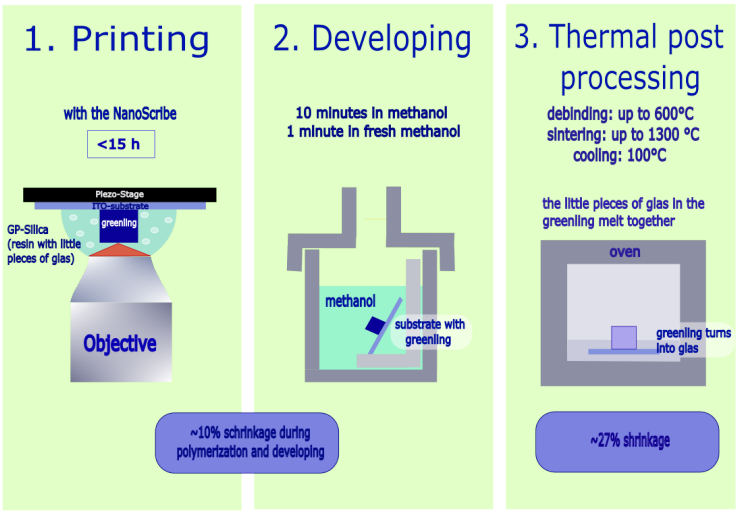

Figure 2.1: Theoretical fabrication process for GP-Silica: First a green part is printed using 3D direct laser-writing, where the liquid resin hardens due to two-photon-polymerisation by a focused laser beam. Then the liquid resin around the green part is washed off with methanol during the developing process. At last the green part is turned into glass by putting it into an oven in the thermal post processing, which consists of a debinding process, a sintering process and a cooling process.

The first step is the printing process. This is done with a commercial 3D direct laser writing system

[1] NanoScribe GmbH & Co. KG: https://www.nanoscribe.com/

- Nanoscribe PPGT+ (see picture 2.2 and 2.3). The resulting greenling (the printed structure out of GP-Silica) is white [12]. Because GP-Silica contains a component that slowly evaporates and so the resin becomes more viscous over time, the printing duration is limited to a maximum of 15 hours and resin stains on mechanical parts should be cleaned off immediately to prevent malfunctions. After about 3 hours the resin will become increasingly sticky and after about 15 hours it will become a gel-like solid [11]. Because the galvo printing mode facilitates high-speed printing [8] and the printing time of the used GP-Silica is limited, the galvo mode is used in this thesis. The resin is actually designed for large sizes (several cubic millimetres), so the 10x objective is recommended [12]. But because the sizes of the wanted membranes are in several micrometer scales, the 63x objective is used. The 63x immersion objective is designed for printing the smallest features possible [13]. During the printing the process can be observed with a live-view camera. When printing with GP-Silica there is typically not a strong contrast in this camera window. A strong contrast can indicate an over-exposed greenling which can lead to cracks in the structure [11].

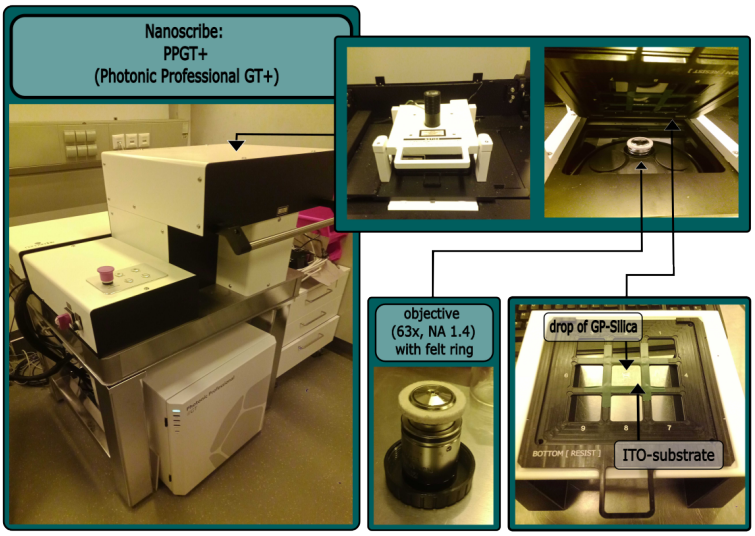

Figure 2.2: Preparation for printing with the Nanoscribe: The 63x objective, that is equipped with a felt ring to prevent the resin creeping into the nosepiece, is placed in the designated place of the optical cabinet. An ITO-coated substrate (ITO: indium-tin oxide [14]) is attached to the substrate holder and a drop of GP-Silica is placed onto the substrate. Then the substrate holder is attached upside down onto a piezo-stage in the optical cabinet.

The second step is the developing of the greenling which removes any un-polymerized liquid resin surrounding the printed structure. Afterwards the objective lens is thoroughly cleaned. For developing the substrate hosting the greenling structure is placed in a 50 ml beaker of methanol for 10 minutes. If the greenling should be detached from the substrate, the methanol bath is followed by a bath with isopropanol for another minute and then can be detached from the substrate. If the greenling should be attached to the substrate, the methanol bath is followed by another bath with fresh methanol for another minute [11]. For fabricating the membranes in the way presented in this thesis the membranes should be attached to the substrate. For preventing the resin from getting viscous the developing step should be done quickly after the completion of a print [11].

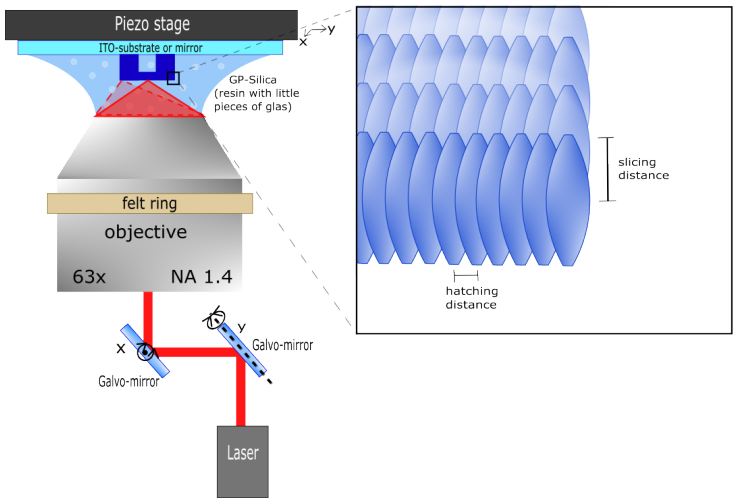

Figure 2.3: Working principle of the Nanoscribe: The objective is dipped into the liquid resin and a pulsed femtosecond fiber laser causes polymerisation of the resin. To be able to print features on a sub-micrometer scale a non-linear two-photon absorption process is used which leads to the production of voxels. The distance between the voxels in the x-y-plane is called hatching distance and the distance between them in the z-axis is called slicing distance. With the piezo printing mode the substrate is moved relative to the laser focus by the piezo-stage. In the galvo printing mode the laser focus is moved in the x-y-plane by two rotatable galvo mirrors and the z-axis is adjustable by the piezo-stage

For cleaning the objective lens, that is contaminated with GP-Silica, methanol is used and the 'dip-in method' is the recommended cleaning procedure [11]. For that a 50 ml beaker is filled with methanol to the position slightly below the 20 ml marker and the objective lens is submerged upside down into the solvent. Only the front lens with the resin should be covered with solvent. The objective should be left in the solvent for a few minutes and then be dried with a ball blower or a nitrogen gun [15]. If a slight whitish residue in the lens gap becomes apparent after the objective cleaning, the residue can be removed by using the 'lens paper method' [11]. For that isopropanol is dropped onto a lens paper and the paper is gently slid over the lens. If required the pressure on the lens can be increased with a cotton stick [15].

The last step is the thermal post-processing, which converts the greenling into glass. It consists of a debinding step with a maximum temperature of $T = 600\,^{\circ}\mathrm{C}$, a sintering step with a maximum temperature of $T = 1\,300\,^{\circ}\mathrm{C}$ and a cooling step with the end temperature of $T = 100\,^{\circ}\mathrm{C}$ followed by turning off the heating and letting it cool down to room-tempreature. The debinding step removes the polymer fraction and the green part becomes a porous brown part, which is then fully turned into fused silica glass by the sintering step. There are two recommended programs (see pictures A.1 and A.2) that are optimised for the oven 'DEKEMA AUSTROMAT 674 with extra vacuum option'[16]. The standard program takes about 60 hours and is used to process structures with a thickness from a few micrometers up to about 1 cm. The fast program takes less than 20 hours and is limited to micron-sized structures [11]. The thermal post process rounds edges which leads to a low shape accuracy [11].

There are two shrinkage phases during the fabrication process. A shrinkage phase of about 10 % overall

can be observed during the polymerisation in the printing process and the development. This shrinkage can be anisotropic. Another shrinkage phase of about 27 % can be observed during the thermal post treatment. This shrinkage is isotropic, if the greenling was detached from the substrate before, and anisotropic, if the greenling kept attached to the substrate [11].

During the sintering step in the thermal post treatment the membranes would be heated up to 1 300 °C. The cavity mirrors, that are used in our fiber microscope, can't withstand these temperatures. To avoid this problem the thermal post processing step with the oven is replaced by a localised laser-based micro-sintering process. For that the CO_2 laser shooting setup of the Bonn Fiber Lab is used. This sintering procedure is presented in chapter 4.

CHAPTER 3

Printing process

The first step for the fabrication of the desired glass membranes with GP-Silica is the printing process as described in the previous chapter. One of the core parts of this thesis is to find working printing parameters for the membranes. The relevant printing parameters, which should be adjusted so that the membranes out of GP-Silica can be printed, are the hatching distance (HD) and slicing distance (SD), the laser power (LP) and the scan-speed (ScSp). The hatching distance describes the distance between the voxels on the x- and y-axis and the slicing distance on the z-axis as shown in picture 2.3. The relative laser power can be adjusted between $LP = 0\%$ and $LP = 100\%$. Other parameters, that can be adjusted, are the size of the structure and the geometry of the structure.

3.1 Finding parameters for cuboids

To get an overview of working regions for the printing parameters cuboids are chosen to be printed because of their simple form. At first different laser powers and scan-speeds are tried out in a 10x10-array of cuboids with the sizes 20 µm x 20 µm x 20 µm, a hatching distance of $HD = 0.2$ µm and a slicing distance of $SD = 0.4$ µm. The recommended hatching and slicing distances for the used 63x objective are $HD = 0.2$ µm and $SD = 0.3$ µm for the resin IP-Dip [13]. The laser power is varied between $LP = 50\%$ and $LP = 95\%$ in steps of 5% and the scan-speed is varied between $ScSp = 1000$ µm/s and $ScSp = 10000$ µm/s in steps of 1000 µm/s. The outcome is shown in picture 3.1 where only the part of the sample is shown with $LP = 65\% - 95\%$ and $ScSp = 6000$ µm/s - 10000 µm/s. It can be seen that the cuboids with too high laser power dissipated or broke off. The cuboids with too low laser power and scan-speed also broke off. For the next prints a scan-speed of $ScSp = 7000$ µm/s and a laser power of $LP = 70\%$ are chosen.

It can be noticed that the cuboids of 3.1 turned out roundish. So in the next print larger sizes are tried out to see, if the edges can be printed sharper with larger sizes. The adjusted sizes are 200 µm x 200 µm x 10 µm, 150 µm x 150 µm x 10 µm, 120 µm x 120 µm x 10 µm, 100 µm x 100 µm x 10 µm and a cylinder with the radius $r = 50$ µm is printed (see picture 3.2). All of the cuboids broke off. The same print is made again (see picture 3.3) but with lower hatching and slicing distances: $HD = 0.1$ µm and $SD = 0.2$ µm. It can be seen that the larger the size the sharper the edges. So GP-Silica has low printing

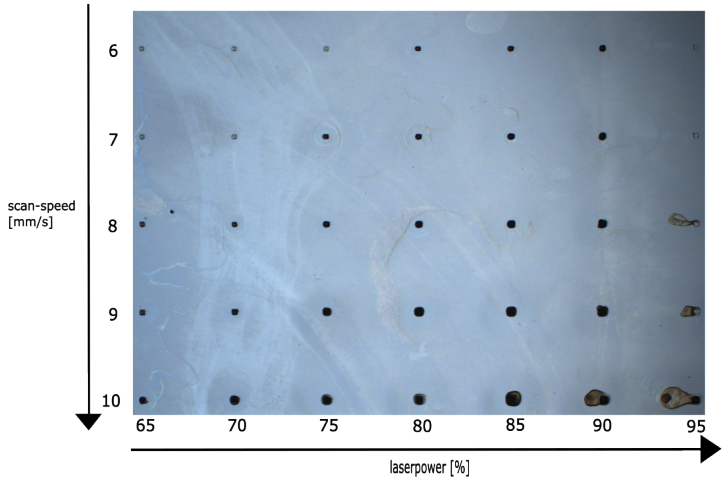

Figure 3.1: printed LP-ScSp-array of GP-Silica cuboids: cuboid size: 20 µm x 20 µm x 20 µm, hatching distance: 0.2 µm, slicing distance: 0.4 µm, laser power: 65% – 90% in steps of 5%, scan-speed: 6000 µm/s - 10000 µm/s in steps of 1000 µm/s; bright field

resolution. Also, a difference in the hatching and slicing distances has a significant effect on the outcome. In the following step these hatching and slicing distances are varied in a HD-SD-array with HD = 0.07 µm - 0.11 µm in steps of 0.01 µm and SD = 0.18 µm -0.22 µm in steps of 0.01 µm (see picture 3.4). The cuboids dissipate with too high hatching and slicing distance. For the next prints the hatching distance HD = 0.08 µm and the slicing distance SD = 0.18 µm of the best result (see picture 3.5) are chosen.

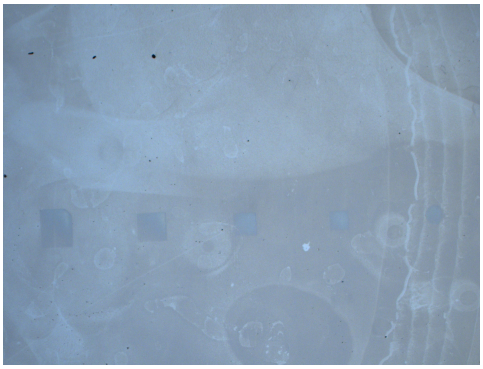

Figure 3.2: printed GP-Silica cuboids of different sizes: height: 10 µm, hatching distance: 0.2 µm, slicing distance: 0.4 µm, laser power: 70%, scan-speed: 7000 µm/s, side lengths: 200 µm x 200 µm, 150 µm x 150 µm, 120 µm x 120 µm, 100 µm x 100 µm, cylinder with radius r = 50 µm; bright field

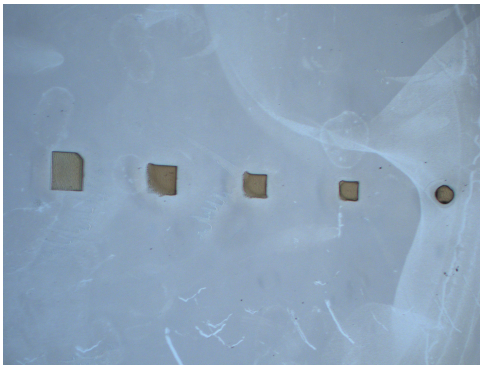

Figure 3.3: printed GP-Silica cuboids of different sizes: height: 10µm, hatching distance: 0.1 µm, slicing distance: 0.2 µm, laser power: 70%, scan-speed: 7000 µm/s, side lengths: 200 µm x 200 µm, 150 µm x 150 µm, 120 µm x 120 µm, 100 µm x 100 µm, cylinder with radius r = 50 µm; bright field

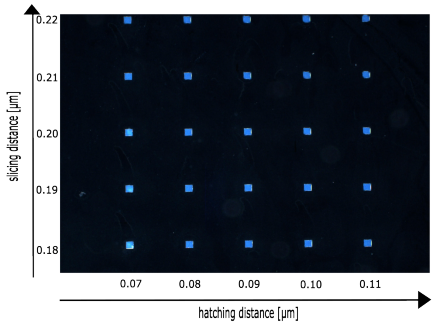

Figure 3.4: printed HD-SD-array of GP-Silica cuboids: cuboid size: 50 µm x 50 µm x 10 µm, hatching distance: 0.07 µm - 0.11 µm in steps of 0.01 µm, slicing distance: 0.18 µm - 0.22 µm in steps of 0.01 µm, laser power: 70%, scan-speed: 7000 µm/s; dark field

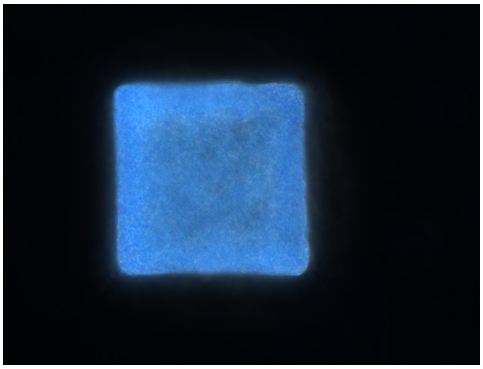

Figure 3.5: best result of 3.4: cuboid size: 50 µm x 50 µm x 10 µm, hatching distance: 0.08 µm, slicing distance: 0.18 µm, laser power: 70%, scan-speed: 7000 µm/s; dark field

With the first found working parameters a 3x3-array of cuboids of the size 145 µm x 145 µm x 10 µm is printed, where all the cuboids have the same printing parameters (see picture 3.6). Compared to the printing duration of the last prints, which were around 2 hours, this print took around 6 hours. The later a cuboid gets printed the more dissipated it gets. This can be caused by the resin getting sticky after around 3 hours [11]. So on the following prints it is ensured that the printing duration does not take longer than 3 hours.

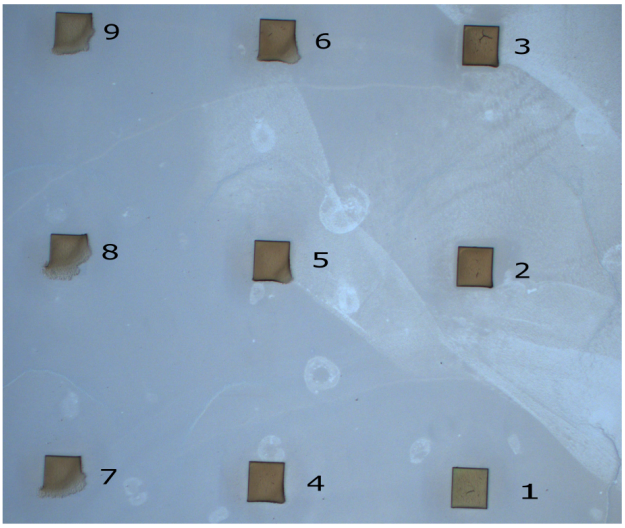

Figure 3.6: printed 3x3-array of GP-Silica cuboids with the same parameters: cuboid size: 145 µm x 145 µm x 10 µm, hatching distance: 0.08 µm, slicing distance: 0.18 µm, laser power: 70%, scan-speed: 7000 µm/s; bright field

3.2 Finding parameters for membranes

After finding printing parameters for the cuboids, working printing parameters for membranes will be figured out. First a simple model for a membrane is used, that consists of two feet at the side edges (3.2.1). Because no working printing parameters for this membrane model could be found, another membrane model, that contains four feet around the corners, is used (3.2.2) for which printing parameters can be found.

3.2.1 Membrane with two feet

The model for the membranes, that is used first, is shown in picture 3.7. It is a square membrane with two feet at the side edges. The size-parameters for this membrane model are the side-length, the feet-height, the feet-width and the thickness of the membrane.

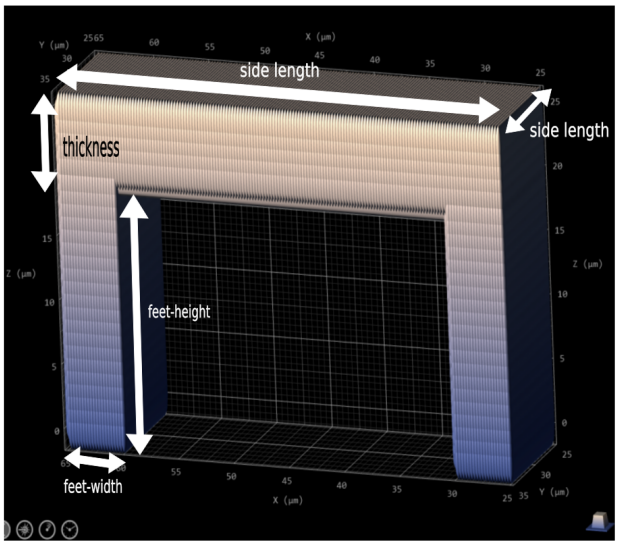

Figure 3.7: DeScribe file of a membrane with two feet with the labelled size-parameters: side-length, feet-height, feet-width and thickness

The printing parameters are set to the parameters that were found for the cuboids and a layer-SD-array can be used to figure out how thin the membrane can be printed (see picture 3.8). One layer has the thickness of the axial resolution of a voxel. The voxel is the smallest printable volume and its size depends on the used objective as well as the used resin. For the 63x objective the lateral resolution of a voxel is $a_{xy} = 340\,\text{nm}$ and the axial resolution is $a_z = 826\,\text{nm}$ [13]. The next layer is printed above the previous layer separated by the slicing distance. In the array the layers are varied from one layer to four layers in the steps of one layer and the slicing distance is varied between $SD = 0.17\,\mu\text{m}$ and $SD = 0.20\,\mu\text{m}$ in steps of $0.01\,\mu\text{m}$. It can be seen that just the feet were printed (see picture 3.8).
Therefore new printing parameters have to be found. Next a LP-ScSp-array - with a membrane thickness of one layer - is printed to check for working printing parameters. The laser power is varied between $LP = 70\%$ and $LP = 100\%$ in steps of 5% and the scan-speed is varied between $ScSp = 6000\,\mu\text{m/s}$ and $ScSp = 13000\,\mu\text{m/s}$ in steps of $1000\,\mu\text{m/s}$. Picture 3.9 shows this array with the laser power of

70% – 100% and the scan-speed of 6000 µm/s - 10000 µm/s. All of the membranes either break in the middle or just their feet remain.
After trying out different combinations of parameters for the laser power (70% – 100%), scan-speed (3000 µm/s - 13000 µm/s), hatching distance (0.045 µm - 0.080 µm), slicing distance (0.16 µm - 0.20 µm) and thickness (1 layer - 7 layers) and not finding working printing parameters, it is tested, if the membranes break during the printing process or during the developing process. In picture 3.10 an LP-ScSp-array of membranes is compared before and after the developing process. It can be seen that the membranes break during the printing process or that just the feet get printed.

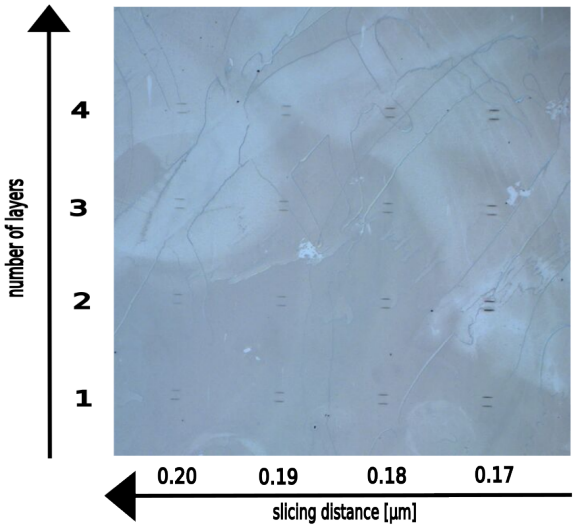

Figure 3.8: printed layer-SD-array of GP-Silica membranes with the parameters: side-length: 40 µm, feet-height: 8 µm, feet-width: 3 µm, thickness: 1-4 layers, hatching distance: 0.08 µm, slicing distance: 0.17 µm - 0.20µm in steps of 0.01 µm, laser power: 70%, scan-speed: 7000 µm/s; bright field

The next approach is to print membranes with much larger thickness. Three LP-ScSp-arrays with the different thicknesses of 2 µm, 2.5 µm and 3 µm are printed with laser powers between $LP = 75\%$ and $LP = 90\%$ in steps of 5% and scan-speeds between $ScSp = 7000$ µm/s and $ScSp = 10000$ µm/s in steps of 1000 µm/s (see picture 3.11). But these membranes cannot be printed either. So another model for the membranes is used, which leads to more stability (3.2.2).

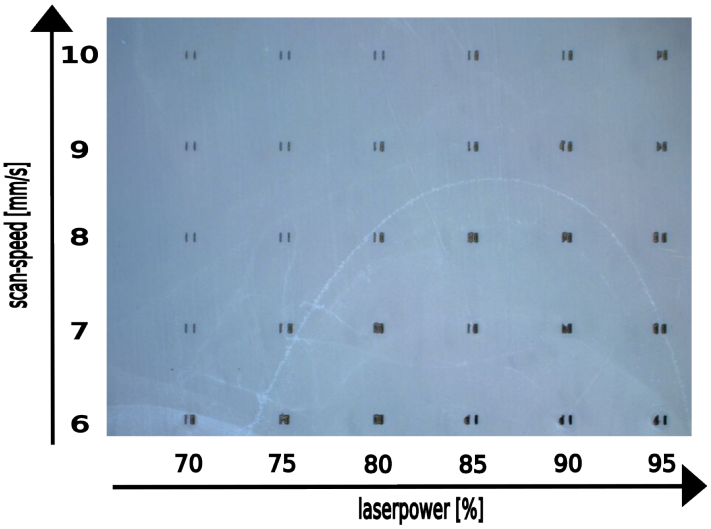

Figure 3.9: printed LP-ScSp-array of GP-Silica membranes with the parameters: side-length: 40 µm, feet-height: 10 µm, feet-width: 5 µm, thickness: 1 layer, hatching distance: 0.08 µm, slicing distance: 0.18 µm, laser power: 70% – 100% in steps of 5%, scan-speed: 6000 µm/s - 10000 µm/s in steps of 1000 µm; bright field

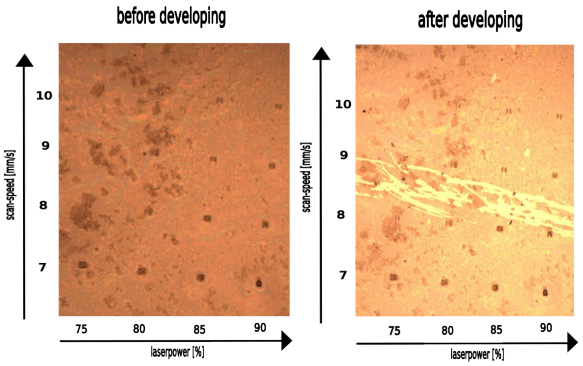

Figure 3.10: printed LP-ScSp-array of GP-Silica membranes before and after development with the parameters: side-length: 30 µm, feet-height: 10 µm, feet-width: 5 µm, thickness: 5 layers, hatching distance: 0.08 µm, slicing distance: 0.18 µm, laser power: 75% – 90% in steps of 5%, scan-speed: 7000 µm/s - 10000 µm/s in steps of 1000 µm/s; bright field

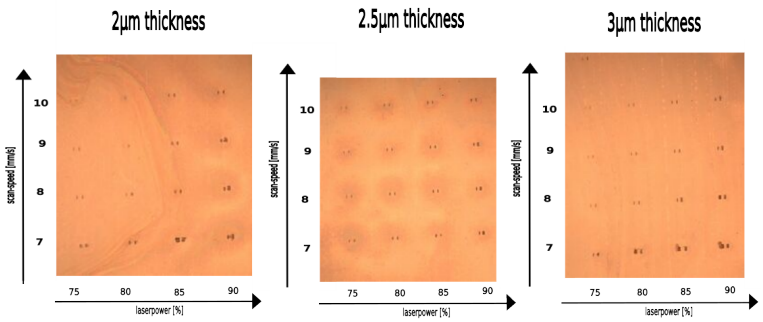

Figure 3.11: printed LP-ScSp-array of GP-Silica membranes with the thicknesses of 2 µm, 2.5 µm and 3 µm with the parameters: side-lengths: 30 µm x 50 µm, feet-height: 10 µm, feet-width: 5 µm, hatching distance: 0.07 µm, slicing distance: 0.18 µm, laser power: 75% – 90% in steps of 5%, scan-speed: 7000 µm/s - 10000 µm/s in steps of 1000 µm/s; bright field

3.2.2 Membrane with four feet around the corners

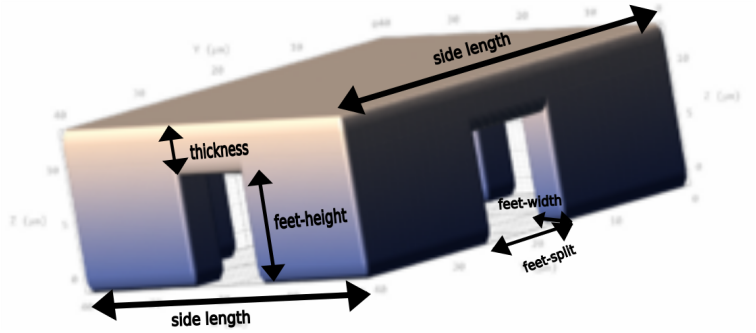

Figure 3.12: DeScribe file of a membrane with four feet around the corners with the labelled size-parameters: side-length, feet-height, feet-width, feet-split and thickness

The new model for the membranes is shown in picture 3.12. It is also a square membrane but it has four feet around the corners. The parameters for this model are the side-length, the feet-height, the feet-width, the feet-split and the thickness of the membrane. Because the membranes of the previous model were breaking in the middle or just the feet were printed, it can be assumed that the shrinkage of the GP-Silica during the polymerisation in the printing process causes the membranes to break in the middle. The new model is symmetric and the feet are holding more parts of the membrane, which should lead to a more stable membrane.
First an LP-ScSp-array of 2µm thick membranes is made for the new model with laser powers between $LP = 70\%$ and $LP = 100\%$ in steps of 10% and with scan-speeds between $ScSp = 7000\,\mu m/s$ and

$ScSp$ = 10000 µm/s in steps of 1000 µm/s (see picture 3.13). It can be seen that in contrast to the previous model the membranes can be printed. The laser powers LP = 85% and LP = 90% in combination with the scan-speeds $ScSp$ = 7000 µm/s and $ScSp$ = 8000 µm/s are leading to the best results. But the membranes are slightly deformed. So an HD-SD-array is made, where the hatching distance of the membranes is varied between HD = 0.04 µm and HD = 0.09 µm in steps of 0.01 µm and the slicing distance of the membrane is varied between SD = 0.14 µm and SD = 0.18 µm in steps of 0.01 µm (see picture 3.14). The hatching and slicing distances of the feet remain at HD_{feet} = 0.08 µm and SD_{feet} = 0.18 µm. It can be seen that the hatching and slicing distances of the membranes have to be lower than the hatching and slicing distances of the feet to get the membrane printed and not just the feet. The best results are achieved with the parameters HD = 0.04 µm and SD = 0.15 µm - SD = 0.17 µm.

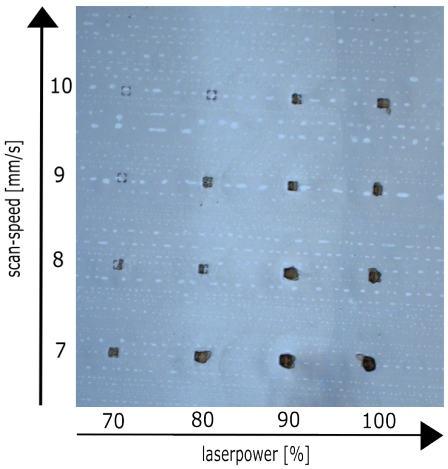

Figure 3.13: printed LP-ScSp-array of GP-Silica membranes with the parameters: side-lengths: 40 µm, feet-height: 10 µm, feet-width: 3 µm, feet-split: 10 µm, thickness 2 µm, hatching distance: 0.07 µm, slicing distance: 0.18 µm, laser power: 70% – 100% in steps of 10%, scan-speed: 7000 µm/s - 10000 µm/s in steps of 1000 µm/s; bright field

The next step is to see how thin the membranes can be printed (see picture 3.15). The thickness is varied from 0.5 µm to 2 µm in the steps of 0.5 µm. The scan-speed is also varied between 7500 µm/s and 8000 µm/s. It can be seen that the membranes should be thicker than 1 µm to be printed well.

After different combinations of the parameters for the laser power (50% – 100%), scan-speed (6000 µm/s - 10000 µm/s), hatching distance of the membrane (0.04 µm - 0.09 µm), slicing distance (0.14 µm - 0.19 µm), thickness (0.5 µm - 10 µm) and side-lengths (40 µm - 150 µm) have been tried out, the following parameters are found to give the best printing results: side-lengths of 100 µm, a thickness of 2 µm, a hatching distance of the feet of 0.08 µm, a slicing distance of the feet of 0.18 µm, a laser power of 85%, a scan-speed of 7500 µm/s, a hatching distance of the membrane of 0.04 µm and a slicing distance of the membrane of 0.15 µm. In picture 3.16 membranes with these parameters are shown. The larger the side-lengths are, the sharper the edges can be printed, but the longer the printing duration gets. So a side-length of 100 μm is used. In the membranes small cracks can be seen. From the e-mail conversation with the Nanoscribe Support it became clear that these cracks can arise during the drying process after the printing and that they can arise in particular with a high energy dose. But no printing parameters

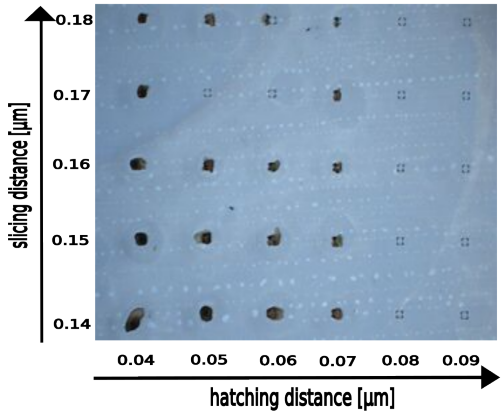

Figure 3.14: printed HD-SD-array of GP-Silica membranes with the parameters: side-lengths: 40 µm, feet-height: 10 µm, feet-width: 3 µm, feet-split: 10 µm, thickness 3 µm, hatching distance of the feet: 0.08 µm, slicing distance of the feet: 0.18 µm, laser power: 85%, scan-speed: 8000 µm/s, hatching distance of the membrane: 0.04 µm - 0.09 µm in steps of 0.01 µm, slicing distance of the membrane: 0.14 µm - 0.18 µm in steps of 0.01 µm; bright field

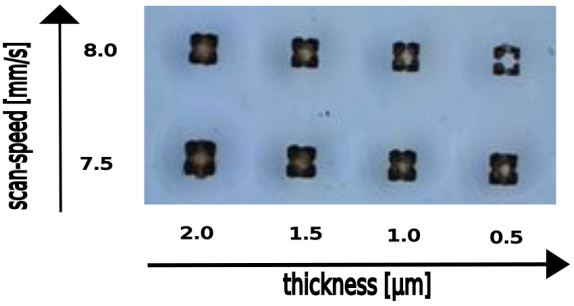

Figure 3.15: printed thickness-ScSp-array of GP-Silica membranes with the parameters: side-lengths: 100 µm, feet-height: 10 µm, feet-width: 15 µm, feet-split: 30 µm, thickness 0.5 µm - 2 µm in steps of 0.5 µm, hatching distance of the feet: 0.08 µm, slicing distance of the feet: 0.18 µm, laser power: 80%, scan-speed: 7500 µm/s - 8000 µm/s, hatching distance of the membrane: 0.04 µm, slicing distance of the membrane: 0.17 µm; bright field

were found without these small cracks.

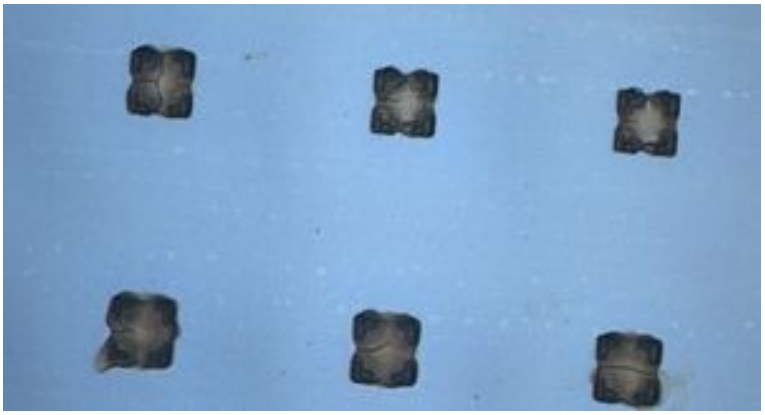

Figure 3.16: printed 2x3-array of GP-Silica membranes with the same parameters: side-lengths: 100 µm, feet-height: 10 µm, feet-width: 15 µm, feet-split: 30 µm, thickness 2 µm, hatching distance of the feet: 0.08 µm, slicing distance of the feet: 0.18 µm, laser power: 85%, scan-speed: 7500 µm/s, hatching distance of the membrane: 0.04 µm, slicing distance of the membrane: 0.15 µm; bright field

3.3 Results

For finding working printing parameters the energy dose of the laser that is required to polymerise the resin is important. The energy dose gets higher with higher laser power and lower scan-speed. When the energy dose is too high, it can lead to overexposure and when the energy dose is too low, it can lead to non-sufficient polymerisation of the resin. With low hatching and slicing distances the voxels can hold together better, but the energy dose gets higher, because neighbouring voxels can receive the laser energy too. Also, the printing duration gets longer with lower hatching and slicing distances. GP-Silica has low printing resolution and so large sizes are leading to sharper edges in the outcome. Large sizes also lead to longer printing duration, which is limited to a maximum of 15 hours [11]. But a maximum of 3 hours is preferred (see picture 3.6). So there is just a small range for the parameters for printing with GP-Silica.
The best found parameters for cuboids are:
a cuboid size of 145 µm x 145 µm x 10 µm, a hatching distance of 0.08 µm, a slicing distance of 0.18 µm, a laser power of 70% and a scan-speed of 7000 µm/s.
And the best parameters for membranes, that could be found, are:
side-lengths of 100 µm, a thickness of 2 µm, a hatching distance of the feet of 0.08 µm, a slicing distance of the feet of 0.18 µm, a laser power of 85%, a scan-speed of 7500 µm/s, a hatching distance of the membrane of 0.04 µm and a slicing distance of the membrane of 0.15 µm.
With these printing parameters there are still small cracks in the membranes, which can be caused by too high energy doses.

CHAPTER 4

Laser-based micro-sintering

The second core part of this thesis is the laser-based micro-sintering of the printed membranes to turn the greenling structures into glass. This is done with the CO_2 laser shooting setup of the Bonn Fiber Lab. In this chapter the working principle of the shooting setup is explained. After that the process of finding shooting parameters to see, if the post thermal process of GP-Silica can be done with the shooting setup, is shown.

4.1 Shooting setup

The construction of the shooting setup is shown in picture 4.1. The installed CO_2 laser gives an output power of 17 W at a wavelength of 9.3 μm. This wavelength is used, because the absorption spectrum for silicon-dioxide glass has a peak at this wavelength with an absorption coefficient of $k = 2$ [17]. The laser light is collimated by a telescope with the focal lengths $f = -50$ mm and $f = 100$ mm. The laser beam is then coupled into a germanium based AOM. The zeroth order is dumped by an air cooled beam dump and the first order is used for shooting. A grid-polarizer with an extinction rate of 1:10000 polarises the light perfectly horizontally. The $\lambda/4$ phase shifting mirror turns the horizontally polarised light into circular polarised light and the laser light is reflected into the final shooting position optics, that contains of a piezo-mirror, a quadrant photo diode, a power meter with a flip-mount and the final shooting lens. With the flip-mount it can be switched between the power meter and the transition through the final shooting lens with $f = 25$ mm [17].
The sample can be attached to a 3D-stage (see picture 4.2). With this 3D-stage the sample can be moved between the focus point of the dual source interferometer and the laser beam for shooting. The distances the 3D-stage has to move between the interferometer and the laser beam can be adjusted with the parameters x_{diff}, y_{diff} and z_{diff} (see picture 4.1).

The parameters for the stage position, for the shooting and for the camera can be adjusted in a graphical user interface (see picture 4.3). The interferometer contains a Mirau objective. In this Mirau objective collimated light from the backside of the objective lens is focused down and falls onto a partially reflected mirror. The reflected fraction of light falls onto a stationary mirror and the transmitted fraction of light falls onto the sample. The reflections of the stationary mirror and the surface are recombined and fall as

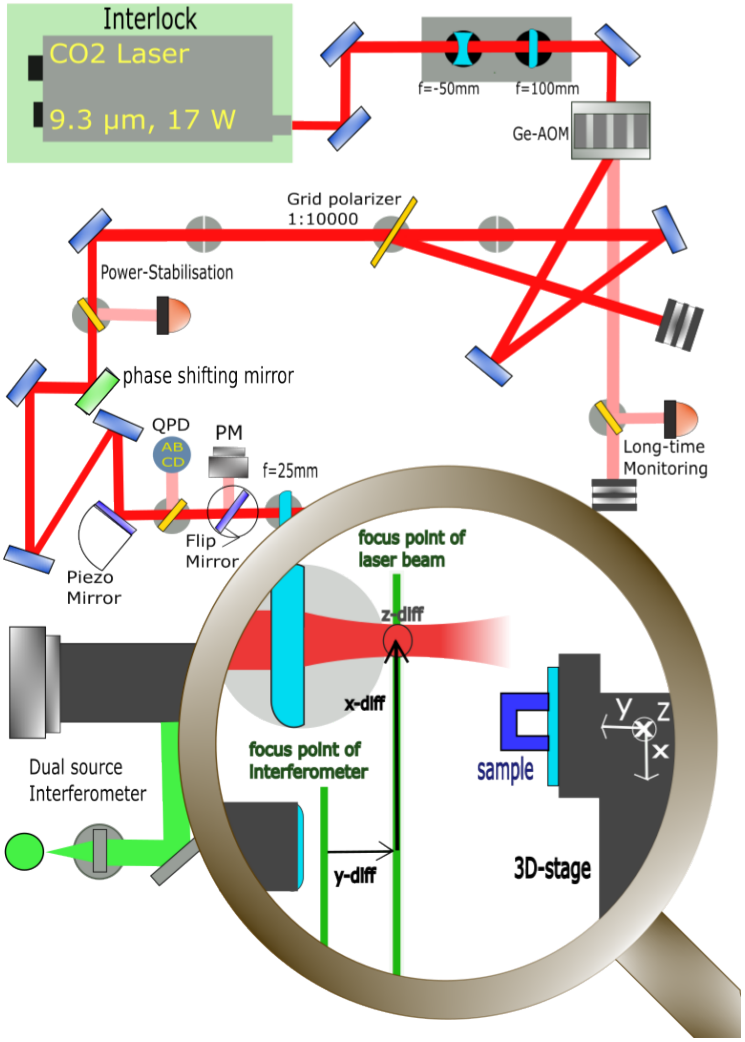

Figure 4.1: sketch of the shooting setup (picture inspired by [17]): The laser light is collimated by a telescope and then coupled into the AOM. For shooting the first order is used and gets horizontally polarised by a grid-polarizer. A phase shifting mirror turns the horizontally polarised light into circular polarised light and the laser light is reflected into the final shooting position optics, that contains of a piezo-mirror, a quadrant photo diode, a power meter and the final shooting lens. The sample can be moved with the 3D-stage between the focus point of the dual source interferometer and the laser beam.

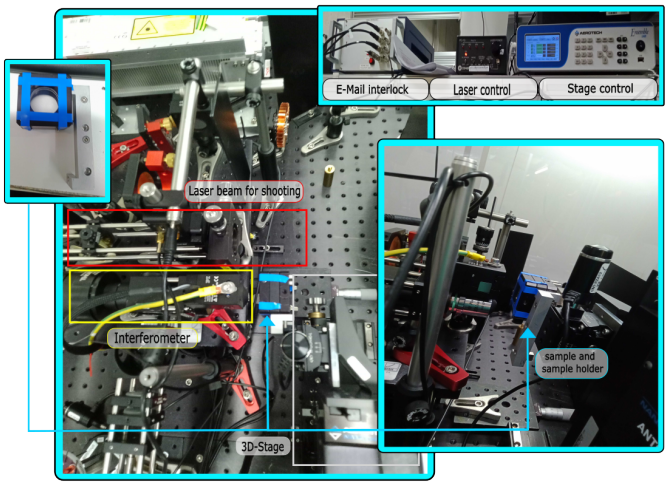

Figure 4.2: picture of the interferometer, the shooting position and the 3D-stage with the attached sample

an overlay back in the objective [18]. This leads to interference fringes in the camera picture. The sample can be rotated around two axis. To get the sample straightly aligned it has to rotate around one axis until the interference fringes are horizontal or vertical and then has to rotate around the other axis until the fringes gets bigger and vanishes. During this alignment it has to be focused by adjusting the parameter y.

Figure 4.3: graphical unit interface to adjust the parameters for the stage position, the shooting and the camera

4.2 Finding parameters

The parameters that can be adjusted for shooting on the membranes are the laser power (P_0), the pulse duration (τ), the number of pulses (n), the delay between pulses (τ_Δ) and the distance (y_{diff}) the 3D-stage moves between the focus point of the interferometer and the position at the laser beam. The pulse duration is the FWHM-time of one pulse, the delay is the time between the pulses and the laser power is the peak power of the pulses (see picture 4.4). So the energy gets higher for higher laser powers, longer pulse duration and higher numbers of pulses. The size of the beam waist can be adjusted by moving the 3D-stage along the propagation line. This is done with the parameter y_{diff}.

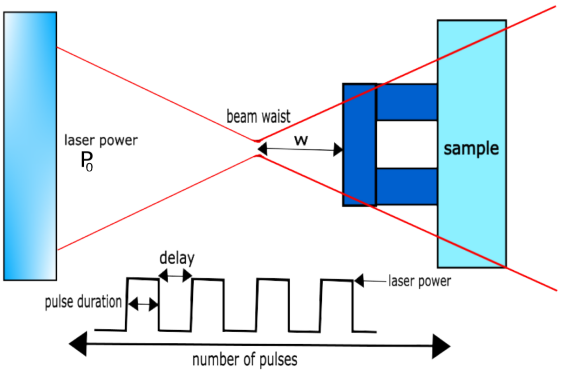

Figure 4.4: Schematic representation of the adjustable parameters in the shooting setup. The parameters laser power, pulse duration, delay between pulses and number of pulses of the pulsed laser are shown. The beam waist at a position w can be adjusted by positioning the sample along the propagation line using the 3D-stage (picture adapted from [17])

4.2.1 First tests with cuboids

To first see, if shooting with the CO_2 laser can replace the post thermal treatment of GP-Silica in the oven, the cuboids are used to shoot on.
Different combinations of the shooting parameters are tried out in the ranges of $\tau = 4\,\text{ms} - 600\,000\,\text{ms}$, $P_0 = 0.05\,\text{W} - 0.5\,\text{W}$, $n = 1 - 50$, $\tau_\Delta = 10\,\text{ms} - 100\,\text{ms}$ and $y_{diff} = 5.184\,\text{mm} - 5.384\,\text{mm}$. Examples of this are shown in pictures 4.5 and 4.6. It can be seen, that some shots turned the greenling into glass. So it is possible to replace the post thermal treatment by using the CO_2 laser. When the laser energy is too low, the greenling does not get fully sintered. When the laser energy is too high, the cuboid can get strongly deformed. The best outcomes are shown in pictures 4.7 and 4.8.

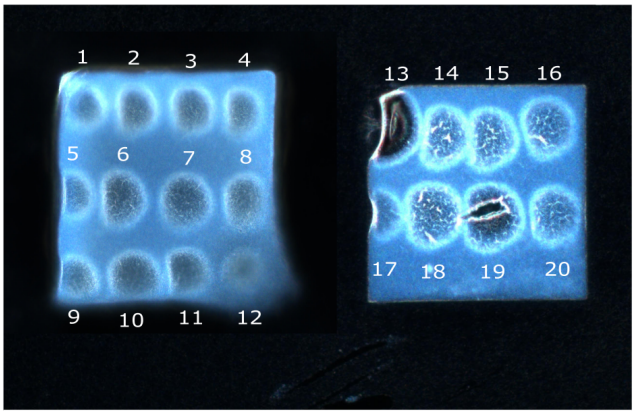

Figure 4.5: on the 145 µm x 145 µm x 10 µm sized cuboids 1 (right) and 5 (left) from 3.6 were shot on with the CO_2 laser with the shooting parameters in A.1, dark field

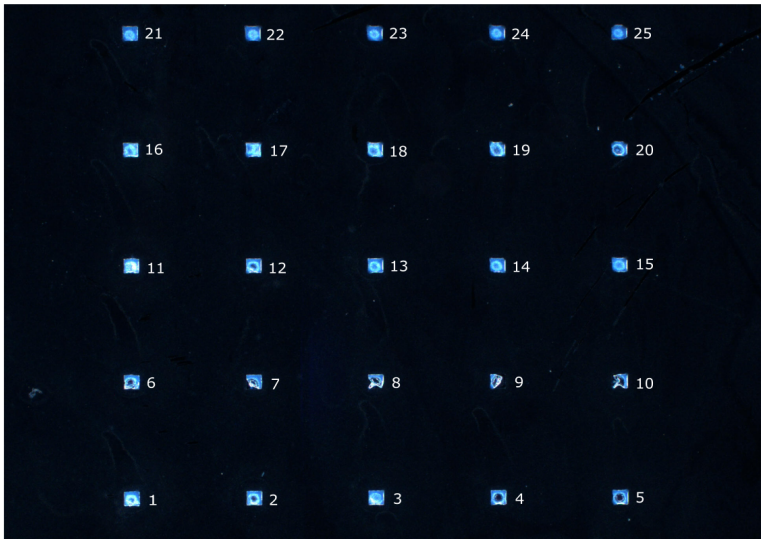

Figure 4.6: on the 50 µm x 50 µm x 10 µm sized cuboids from 3.4 were shot on with the CO_2 laser with the shooting parameters in A.2, dark field

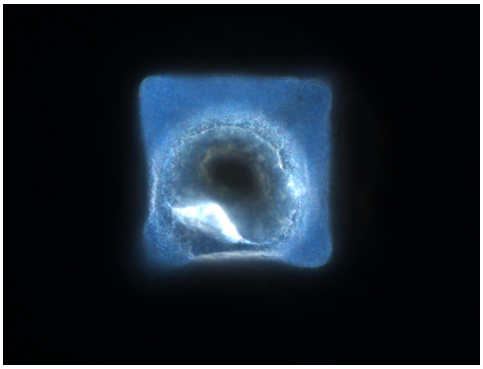

Figure 4.7: cuboid 12 from 4.6 with the shooting parameters: $\tau = 8\,\text{ms}$, $P_0 = 0.12\,\text{W}$, $n = 20$, $\tau_\Delta = 100\,\text{ms}$ and $y_{diff} = 5.284\,\text{mm}$, dark field

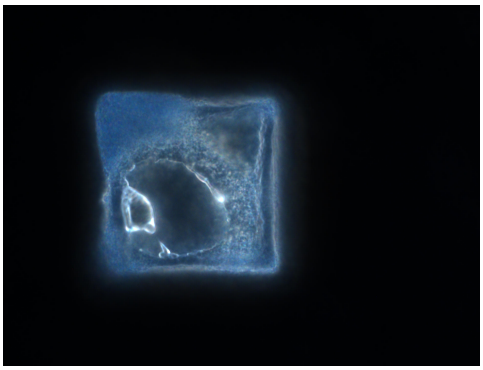

Figure 4.8: cuboid 12 from 4.6 with the shooting parameters: $\tau = 8\,\text{ms}$, $P_0 = 0.15\,\text{W}$, $n = 1$ and $y_{diff} = 5.284\,\text{mm}$, dark field

4.2.2 Parameters for membranes

To get an idea for the shooting parameters for the membranes different combinations of $P_0 = 0.05\,\text{W} - 0.70\,\text{W}$, $\tau = 2.5\,\text{ms} - 60.0\,\text{ms}$, $\tau_\Delta = 10\,\text{ms} - 2\,000\,\text{ms}$, $n = 5 - 10$ and $y_{diff} = 5.39\,\text{mm} - 5.88\,\text{mm}$ are tried out. Some examples are shown in pictures 4.9, 4.10, 4.11 and 4.12. It can be seen, that the beam radius could be adjusted with the parameter y_{diff}. When the energy is too high, the membrane becomes glass but also shrinks to the feet so that just the feet are left (see 4.9).

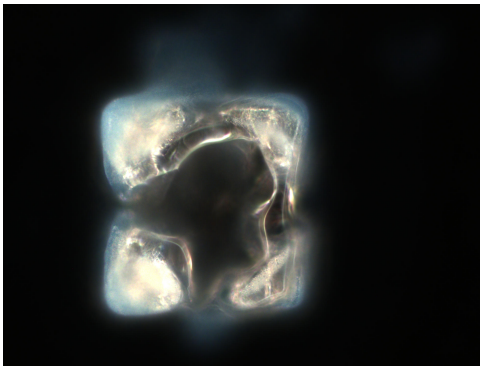

Figure 4.9: membrane with the side-length 100 µm, the feet-height 10 µm, the thickness 2 µm and with the shooting parameters: $\tau = 8\,\text{ms}$, $P_0 = 0.6\,\text{W}$, $n = 5$, $\tau_\Delta = 100\,\text{ms}$ and $y_{diff} = 5.75\,\text{mm}$; printing parameters in A.4; dark field

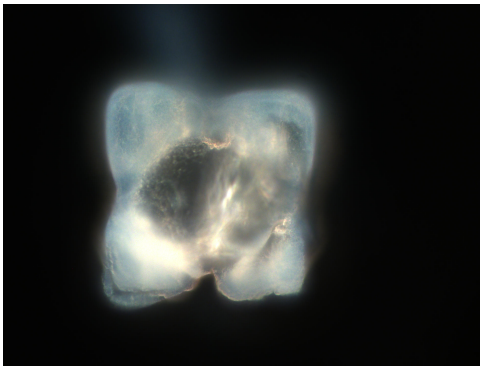

Figure 4.10: membrane with the side-length 100 µm, the feet-height 10 µm, the thickness 2.2 µm and with the shooting parameters: $\tau = 8\,\text{ms}$, $P_0 = 0.2\,\text{W}$, $n = 5$, $\tau_\Delta = 100\,\text{ms}$ and $y_{diff} = 5.775\,\text{mm}$; printing parameters in A.4; dark field

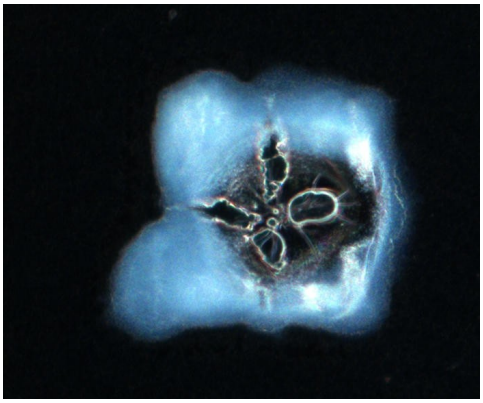

Figure 4.11: membrane with the side-length 100 µm, the feet-height 10 µm, the thickness 2 µm and with the shooting parameters: τ = 8 ms, P_0 = 0.35 W, n = 5, τ_Δ = 100 ms and y_{diff} = 5.5 mm; printing parameters in A.4; dark field

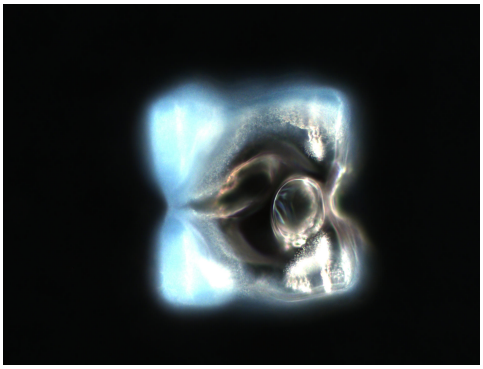

Figure 4.12: membrane with the side-length 100 µm, the feet-height 10 µm, the thickness 2 µm and with the shooting parameters: τ = 8 ms, P_0 = 0.4 W and then shooting again with P_0 = 0.575 W, n = 5, τ_Δ = 100 ms, y_{diff} = 5.7 mm, P_0 = 0.4 W and then shooting again with P_0 = 0.575 W; printing parameters in A.4; dark field

When the energy is too low, the membrane does not get fully sintered (see 4.10). Also it can be seen that big cracks in the membranes are being formed (see 4.11) or air bubbles are getting sealed in (see 4.12). The next step is to try to shoot on all four corners and in the middle of the membranes instead of just shooting in the middle to get them fully sintered. But this procedure leads to big cracks in the membranes (see picture 4.13). A reason for this is the long time between the shots, so the shrinkage can happen before the new shot in the next corner is done.

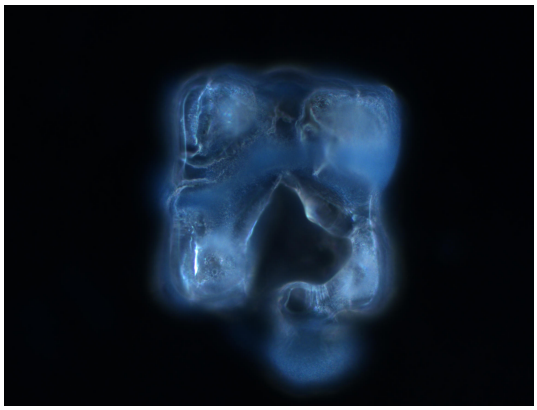

Figure 4.13: membrane with the side-length 100 µm, the feet-height 10 µm, the thickness 2.2 µm and with the shooting parameters on all four corners: τ = 8 ms, P_0 = 0.35 W, n = 5, τ_Δ = 100 ms and y_{diff} = 5.7 mm and one shot in the middle with P_0 = 0.1 W; printing parameters in A.4; dark field

To prevent these cracks the delay between the pulses has to be adjusted. With a long delay the membranes can be cooled down between the pulses, which can then lead to cracks. With a short delay the energy of one pulse can get too high, which can also lead to cracks. The time a cuboid of

glass needs to cool down through heat radiation can be estimated by using the Stefan-Boltzmann-law [19]:

$$\frac{dT}{dt} = -\frac{\epsilon\sigma A}{mc} \cdot (T^4 - T_U^4) = a \cdot (T^4 - T_U^4) \tag{4.1}$$

with temperature T, time t, mass m, specific heat capacity c, emissivity ϵ, Stefan Boltzmann constant σ, surface A of the glass, temperature T_0 at the beginning, temperature T_U of the surrounding and $a = -\frac{\epsilon\sigma A}{mc}$.
This differential equation can be solved numerically (see pictures 4.14 and 4.15). As a first estimation the following values are used:
$\epsilon = 1$, $c_{glas} = 840 J k g^{-1} K^{-1}$ [20], $\sigma = 5.67 \cdot 10^{-8} W m^{-2} K^{-4}$ [19], $m = \rho V$ [20] with the volume V for the size 100 µm x 100 µm x 10 µm and the density $\rho_{glas} = 25000 k g m^{-3}$ [21].

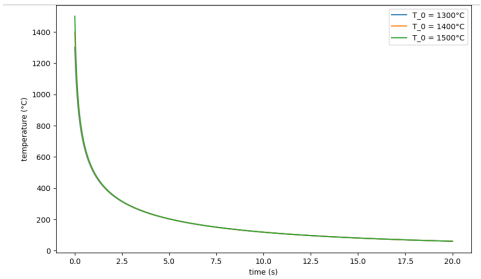

Figure 4.14: cool down through heat radiation; numerical solution of the equation 4.1

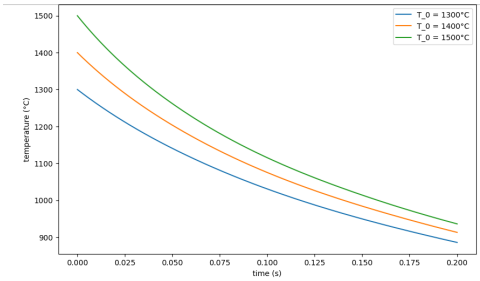

Figure 4.15: cool down through heat radiation; numerical solution of the equation 4.1

In pictures 4.14 and 4.15 it can be seen that the cool down time for glass cuboids of the size 100 µm x 100 µm x 10 µm is on the seconds scale. In the range of 0 ms – 200 ms the temperature is cooling down fast. So the delay between the pulses is varied between $\tau_\Delta = 1$ ms and $\tau_\Delta = 170$ ms with the number of pulses $n = 2$ for the shooting parameters of 4.10 to find the best adjustment for the delay. These shooting parameters are used, because with these parameters no cracks occur. The results for the different delays are shown in picture 4.16. The longer the delay is, the more the membrane gets sintered and the more cracks are occurring. With short delays there are also cracks. The delays that lead to the least amount of cracks are $\tau_\Delta = 16$ ms and $\tau_\Delta = 20$ ms. For the delay $\tau_\Delta = 18$ ms an increase in the number of pulses is used to attempt to turn the membrane into glass without cracks (see picture 4.17). But it can be seen that more cracks occur with more pulses. So another method to prevent the cracks is needed.

For finding another method to prevent cracks occurring in the membranes the recommended post thermal treatment is considered further. The temperature in the debinding process is increased gradually with multiple holding periods until 600 °C is reached (see 4.18, 4.19). In this debinding step the polymer gets burned and the greenling becomes a brownling. This brownling consists of fused silica glass in the form of nano particles, which are held together by the few rests of polymer. If the debinding process is too fast, the structure can be damaged in form of cracks and explosions. In the sintering process the brownling turns into the final glass part through removal of the rest polymer and the merging of the nano particles. In this step the shrinkage takes place[1]. After that the cooling process begins.

[1] Information acquired by an e-mail exchange with the Nanoscribe Support

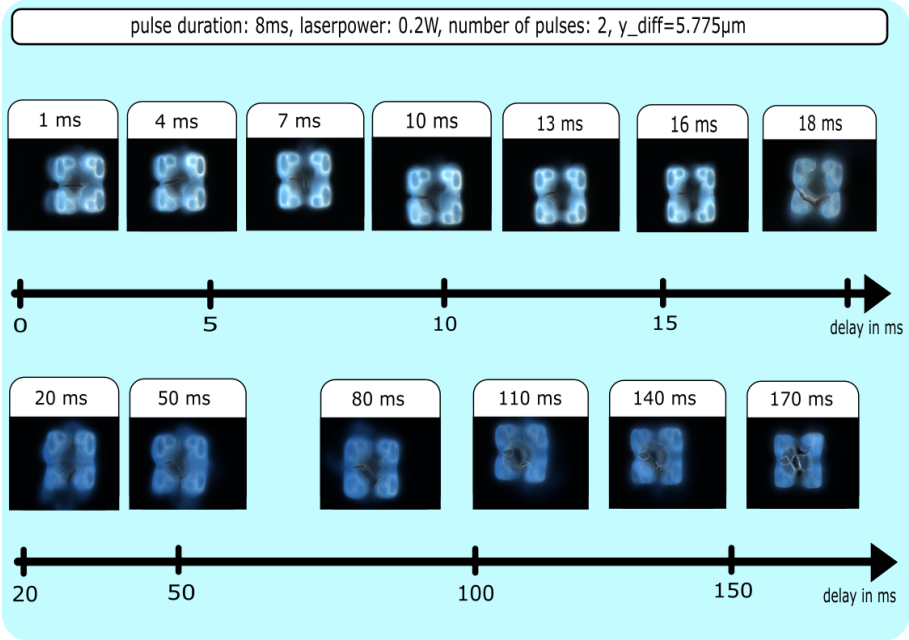

Figure 4.16: shooting on membranes with side-lengths of 100 µm, feet-heights 10 µm, thicknesses 2.2 µm and with the shooting parameters: $\tau = 8$ ms, $P_0 = 0.2$ W, $n = 2$, $\tau_\Delta = 1$ ms − 170 ms and $y_{diff} = 5.775$ mm; printing parameters in A.4; dark field

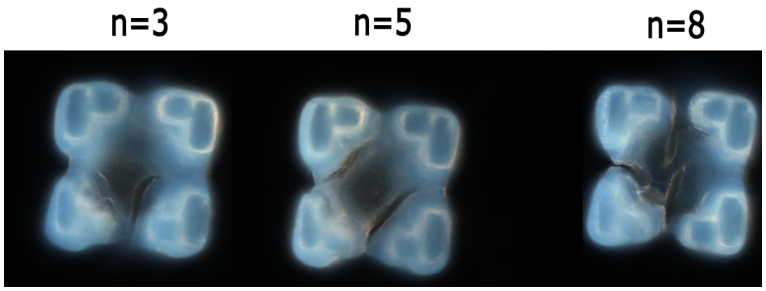

Figure 4.17: shooting on membranes with side-lengths of 100 µm, feet-heights 10 µm, thicknesses 2.2 µm and with the shooting parameters: $\tau = 8$ ms, $P_0 = 0.2$ W, $n = 3 - 8$, $\tau_\Delta = 18$ ms and $y_{diff} = 5.775$ mm; printing parameters in A.4; dark field

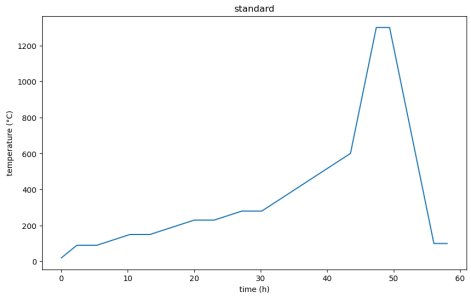

Figure 4.18: Temperature of the GP-Silica standard thermal processing program A.1 against time

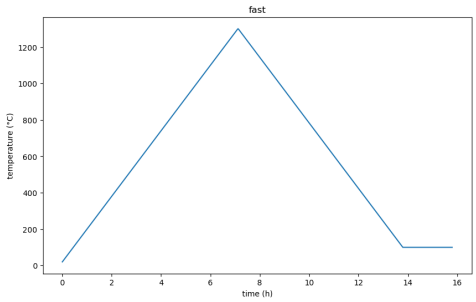

Figure 4.19: Temperature of the GP-Silica fast thermal processing program A.2 against time

To prevent cracks in the membranes the debinding process and cooling process are imitated by placing shots with lower laser power before and after the shots with the set laser power. In the graphical user interface of the shooting setup only a constant laser power can be set (see picture 4.3) and the time between multiple shots with different settings for the laser power would take too long, so that it could lead to cracks. So an extension to the python code is done for increasing and decreasing the laser power during the pulses in one shot. The important part of the python code for implementing this code extension is the definition of the shoot button and the function $sample\_pulse$, that is shown in picture 4.20. All the important information about the voltage for the AOM over the shooting time is situated in $data$. The array $data$ is created by the function $sample\_pulse$, that needs the parameter for the length of one pulse (on_time), which is the pulse duration, the parameter for the time between the pulses (off_time), which is the delay between pulses, and the parameter for the voltage of the AOM (amp). In the function $sample\_pulse$ the AOM voltage is multiplied by an array out of ones and the result of this is the array on.
For increasing and decreasing the laser power during the shot the parameter amp that is given to the function for the AOM voltage is changed. Instead of the set AOM voltage an array in the length of the array on is created and then filled with the voltage values that are supposed to be tested. In picture 4.21 the written python code is shown. In this example the array is split up in five parts with the same lengths and the first and last part are filled with 50% of the set AOM voltage and the three middle parts are filled with the set AOM voltage. The new $data$ then can be commented in and the previous $data$ can be commented out to get the laser power during the shooting with the AOM voltages as adjusted in the array. If the new $data$ is not commented in, the shooting button works like before.

In picture 4.22 a comparison between a shot with a constant laser power and shots with pulses of lower laser power before and after is shown. The membrane, that was shot on with constant laser power, has cracks in contrast to the other membranes, that have been shot on with pulses of lower laser power before and after. The delay was set to $\tau_\Delta = 100\,\text{ms}$ to get a better comparison. So cracks in the membranes can be prevented with this method.
The debinding step is the essential part to prevent cracks. If only pulses with lower laser power are put after the shot, cracks are occurring as well (see membranes 8 and 9 of picture 5.4).

```
def sample_pulse(self, on_time, off_time, amp):
    on = np.ones(int(round(self.samples_per_second*on_time)))*amp
    off = np.zeros(int(round(self.samples_per_second*off_time)))
    return np.concatenate((on,off)) + self.ofset_voltage

def shoot_button(self):
    """ Sets the shooting voltage waveform to the BNC board"""
    with ni.Task() as analogue_task, ni.Task() as trig_task, ni.Task() as gate_task:
        print("Shooting...", end = "\r")

        time_for_shooting=int(self.no_of_pulses*(self.delay_bw_pulses+self.pulse_duration)+10)
        analogue_task.ao_channels.add_ao_voltage_chan(self.analog_channel_aom)
        trig_task.co_channels.add_co_pulse_chan_time(self.trig_chan_generation,
        high_time=self.pulse_duration, low_time=self.delay_bw_pulses)

        data=self.sample_pulse(self.pulse_duration, self.delay_bw_pulses, self.aom_voltage)
        #-------------------------------------------------------------------------------
```

Figure 4.20: part of the python script that is important for implementing the python code extension for increasing and decreasing the laser power during one shot with multiple pulses

```
#-------------------------------------------------------------------------------
#laserpower increases and decreases with the number of pulses: cool down "curve"
#written by Johanna

#array of amplitudes(aom_voltage) in the length of "on"(sample_pulse):
amp_cool_down = np.zeros(int(round(self.samples_per_second*self.pulse_duration)))
l = len(amp_cool_down) #array length
l1 = int(math.floor(l/5)) #length of 20% of the array length
for i in range(0, l1-1, 1):
    amp_cool_down[i] = 0.5*self.aom_voltage
for i in range(l1, 4*l1-1, 1):
    amp_cool_down[i] = self.aom_voltage
for i in range(4*l1, 5*l1-1, 1):
    amp_cool_down[i] = 0.5*self.aom_voltage
#comment this in and the other data out for a laserpower ramp
#data=self.sample_pulse(self.pulse_duration, self.delay_bw_pulses, amp_cool_down)
#-------------------------------------------------------------------------------
```

Figure 4.21: python code extension for increasing and decreasing the laser power during one shot with multiple pulses

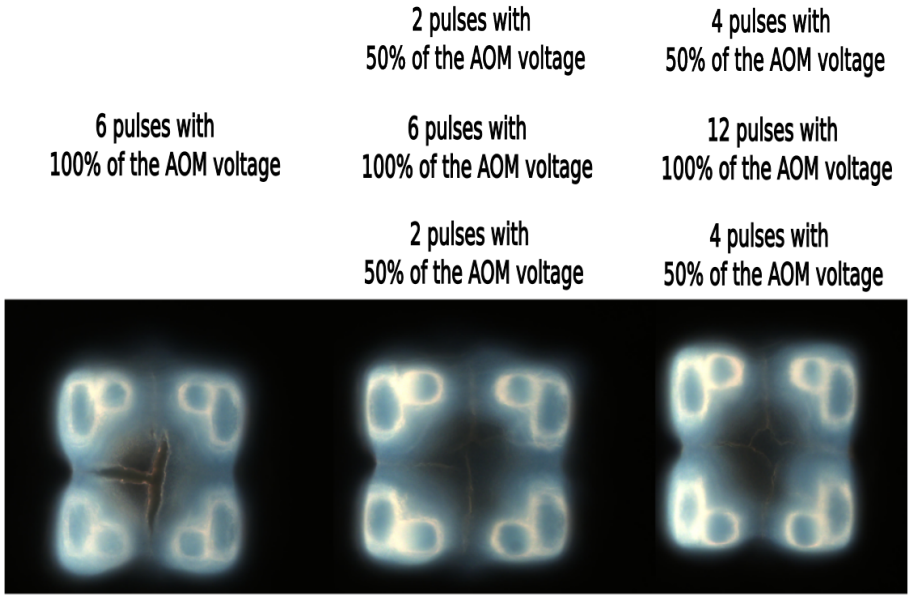

Figure 4.22: shooting on membranes with side-lengths of 100 µm, feet-heights 10 µm, thicknesses 2.2 µm and with the shooting parameters: $\tau = 8$ ms, $P_0 = 0.2$ W, $\tau_\Delta = 100$ ms and $y_{diff} = 5.775$ mm; printing parameters in A.4; dark field

4.3 Results

In this chapter it was shown that it is possible to use the shooting setup for the post thermal processing of membranes out of GP-Silica. With too low laser energy the membranes do not get fully sintered and with too high energy they shrink, so that just the feet are left over. A problem that occurs are cracks in the membranes. These can be caused by a too short or a too long delay between the pulses. Cracks can also occur with a too short debinding and cooling process. So they can be prevented by placing pulses with lower laser power before and after the pulses with the highest laser power. Optimal shooting parameters have not been found yet. As it is not yet clear, if the membranes with the pulses before and after with lower laser power (see picture 4.22) turn into glass or become very thin, the measuring of the coupling depth is dealt with in the next chapter 5.

CHAPTER 5

Measuring the coupling depth

In this chapter the coupling depth of the membranes, manufactured according to the parameters in the previous chapters (3, 4), is experimentally investigated. The coupling depth describes the reduction in the reflection signal of an optical cavity on resonance and can be an indirect proxy of membrane quality [18]. For that a device called the "Vacuum fiber microscope" is used (the vacuum part is irrelevant for the discusssion here) (see picture 5.2). It can precisely position fiber mirrors (optical fibers coated with a Bragg reflector) over a mirror substrate for cavity construction. An overview of the working principle of the fiber microscope is shown in picture 5.1.

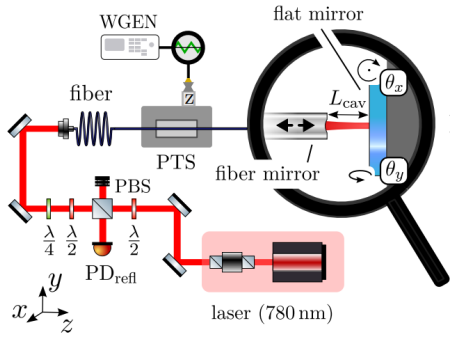

Figure 5.1: Sketch of the fiber microscope for the measurement of the coupling depth: The laser light is led into a Polarizing-Beam-Spliter (PBS) and is then coupled into a hybrid fiber cavity, that consists of the in-coupling fiber mirror and a flat mirror with the mechanical resonators (membranes) on it. The cavity length can be scanned with a Piezo-Translation-Stage (PTS). The signal of the back-reflected light is recorded with a photo diode (PD_{refl}) [18]

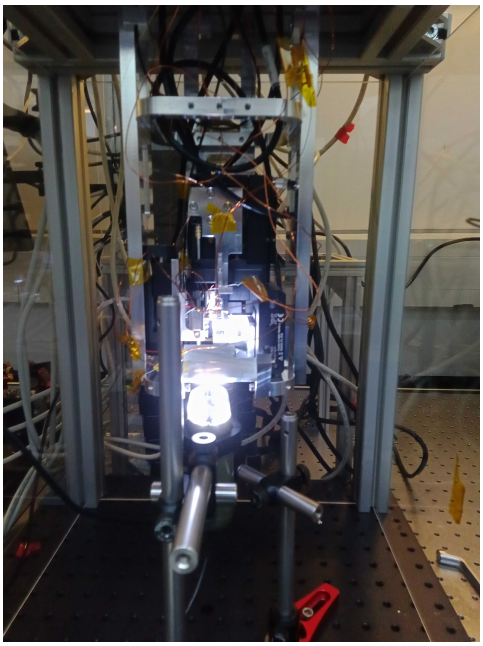

Figure 5.2: Photo of the fiber microscope

The laser light of a wavelength tunable laser, that is set to $\lambda = 780\,\mathrm{nm}$, with an output power of 20 mW is

led to a Polarizing-Beam-Splitter (PBS) and is then coupled by the in-coupling fiber mirror into a hybrid cavity. The hybrid cavity consists of the fiber mirror and a macroscopic flat mirror with the membranes on it. Wave plates before and after the PBS ensure that the back-reflected light is rotated by 90° and then arrives at the photo diode. The cavity gets resonant, when the cavity length is $L_{cav} = \frac{\lambda}{2}$. The reflected light then interferes destructively with the field that is leaking back out of the cavity. The power, that is measured with the photo diode, reduces by the coupling depth of the cavity [18]. The coupling depth measures the fraction of light coupled into the cavity mode relative to the total input [9]. In the ideal resonance case the power should become zero. The z-position of the fiber mirror and so the cavity length is scanned with a Piezo-Translation-Stage (PTS) to get this resonance [18]. Further information about the fiber microscope can be found in [18] and [22].
To install the membranes in the experiment they have to be printed on a flat mirror that is then used as a cavity mirror in the hybrid (fiber+substrate) cavity setup. A DBR (distributed bragg reflector) -mirror with 2000ppm transmission is used for this. The membranes can be printed with the same parameters as on the ITO-substrates (see picture 5.3).

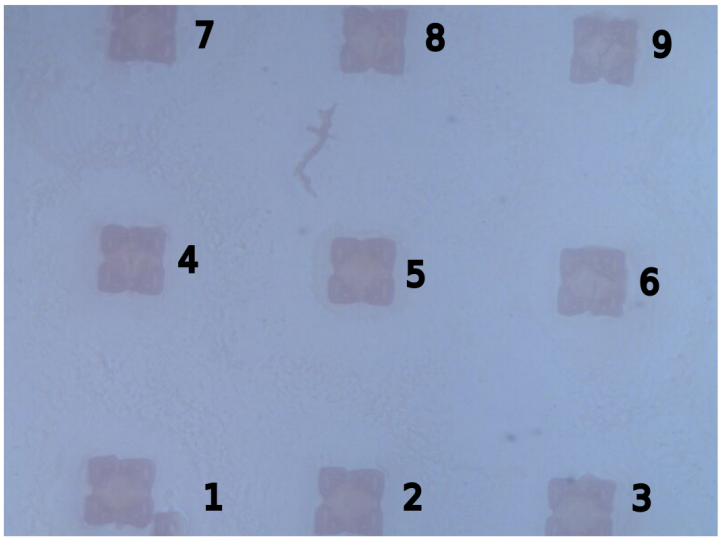

Figure 5.3: printed 3x3-array of GP-Silica membranes with the same printing parameters: side-lengths: 100 µm, feet-height: 10 µm, feet-width: 15 µm, feet-split: 30 µm, thickness 2.2 µm, hatching distance of the feet: 0.08 µm, slicing distance of the feet: 0.18 µm, hatching distance of the membrane: 0.04 µm, slicing distance of the membrane: 0.15 µm, laser power: 85%, scan-speed: 7500 µm/s; bright field

Next they are shot on with different combinations of CO_2 laser pulses to see, if the membranes are turning into glass, or, if their thickness just reduces. Then the mirror, with the membranes on it, is placed into the experiment and the fiber mirror is positioned above it (see pictures 5.5 and 5.6).
The results of the measurement are shown in picture 5.7. Also the coupling depth is measured on the marker structure of the array (the printing parameters are the same as of the other membranes of 5.3 but with the side-lengths 50 µm, feet-height: 10 µm, feet-width: 5 µm, feet-split: 15 µm, thickness 2 µm) (see picture 5.8). The marker is printed on the arrays to be able to assign the membranes and it is not shot on the marker. On a place of the mirror without membranes the coupling depth is measured as well (see picture 5.9).

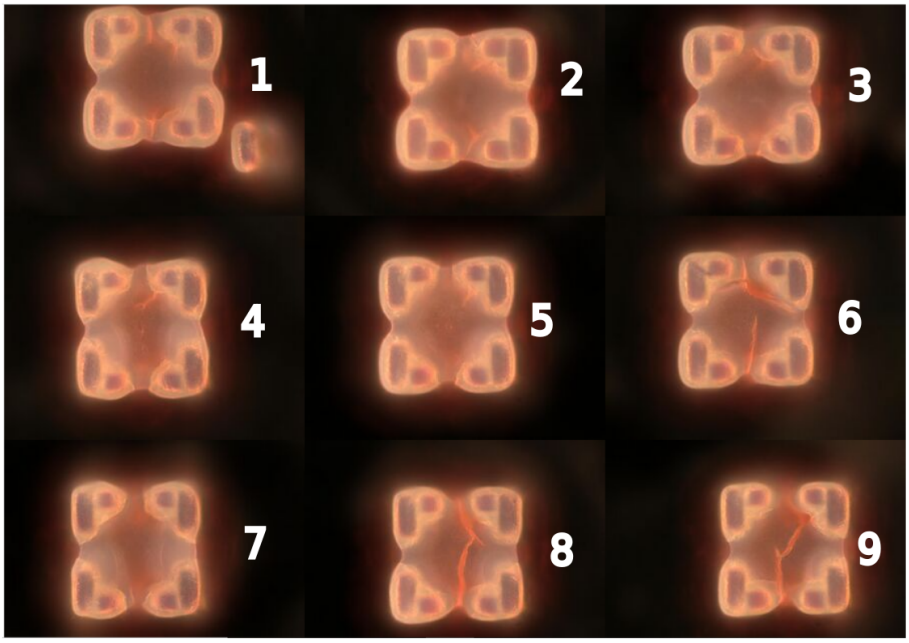

Figure 5.4: membranes of 5.3 that are shot on with the shooting parameters of A.3; dark field

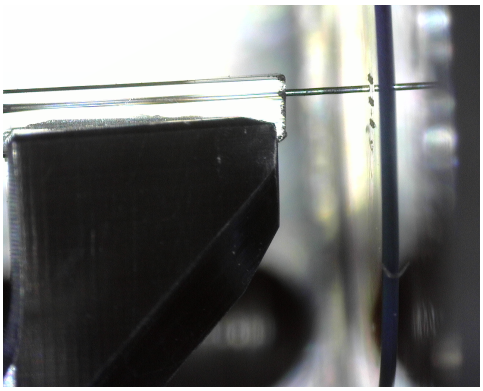

Figure 5.5: Adjusting the fiber mirror above the membranes on the flat mirror, view from the side

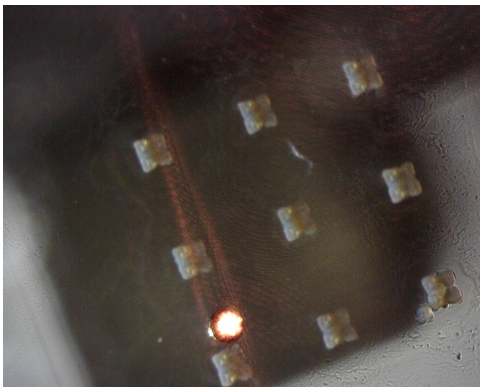

Figure 5.6: Adjusting the fiber mirror above the membranes on the flat mirror, view through the flat mirror

It can be seen that the measured coupling depth is comparatively low. The coupling depth of a well-fabricated fiber mirror with proper cavity mode-matching can reach up to 95% [18]. The coupling depth of an average membrane made from the resin IP-S is about 20 % [9]. This is also approximately the threshold from where a membrane becomes useful for the experiment. The measurement of the coupling depth on the mirror without membranes shows, that the coupling depth is below 30% for some spots on the mirror and the coupling depth with the membranes is below 5%. A reason for this could be that after the developing process stains of GP-Silica are left on the substrate. They

can be removed by isopropanol but that could detach the membranes from the substrate. Because the coupling depth is low due to these GP-Silica stains on the mirror, it is not possible to determine if the membranes of picture 5.4 turned into smooth glass or just became thinner. But it can be seen that the higher coupling depths measured with the membranes are distributed over a larger area of the membrane than the higher coupling depths measured with the marker-structure, that was not shot on.

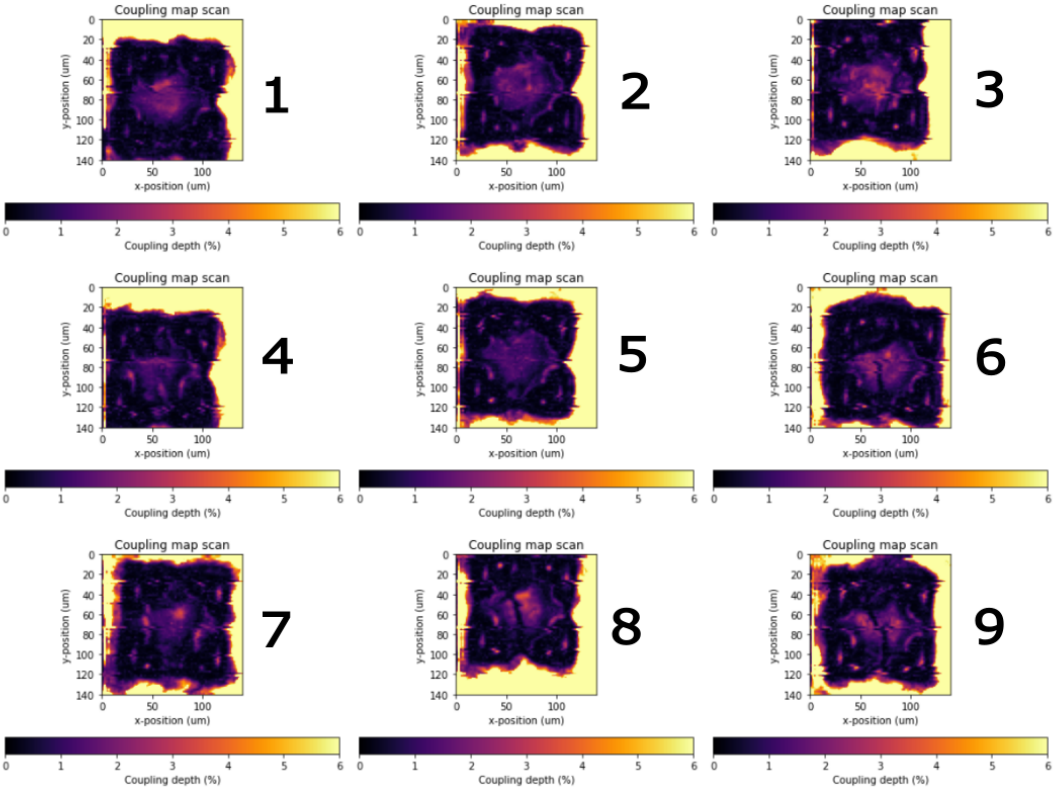

Figure 5.7: Measurement of the coupling depth with the membranes from 5.4 with the wavelength $\lambda = 780\,\text{nm}$

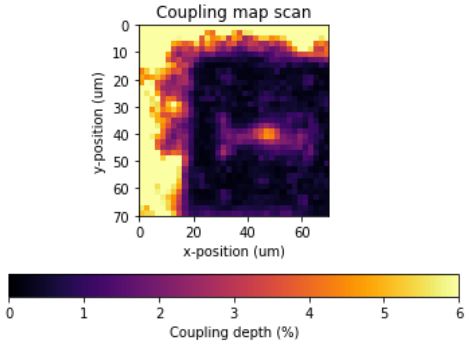

Figure 5.8: Measurement of the coupling depth with the marker of the membrane-array from 5.4 with the wavelength $\lambda = 780\,\text{nm}$

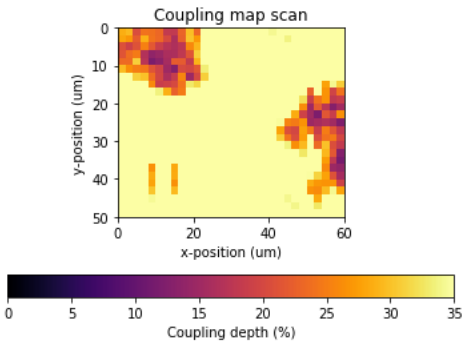

Figure 5.9: Measurement of the coupling depth at a place on the mirror without membranes with the wavelength $\lambda = 780\,\text{nm}$

CHAPTER 6

Conclusion and Outlook

The purpose of this thesis was to explore, if membranes out of GP-Silica can be fabricated using laser-based micro-sintering instead of the recommended post thermal treatment in an oven. Here I demonstrated that this is indeed possible.
Working printing parameters for GP-Silica with using the 63x objective had to be found. It was shown that GP-Silica has lower printing resolution than previous used resist and this complication was circumvented by larger sizes of the membranes. Notably, I found that the printing duration should be below 3 hours to get good results.
The second core part was to find suitable shooting parameters with the CO_2 shooting setup. Although the shooting parameters can still be further optimised, it could be verified, that it is possible to use the shooting setup for turning the membranes into glass. A way to prevent cracks occurring in the membranes was found by placing shots with lower laser power before and after the shots with higher laser power.
Because of left GP-Silica stains on the substrates after the developing process, a comparison of the coupling depth and the resulting Q-factor between the membranes made of GP-Silica and the other membranes out of IP-S could not be done yet.
Challenges, that still need to be solved, are the cracking of the membranes, the measuring of the optical finesse and the measuring of the Q-factor.

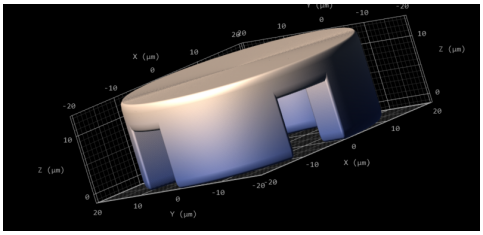

Figure 6.1: DeScribe file of a round membrane with four cuts in the feet

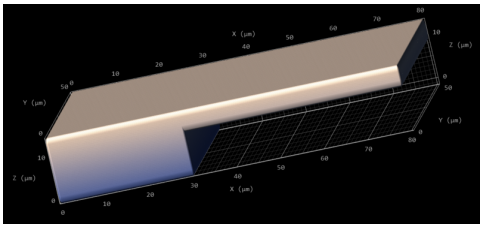

Figure 6.2: DeScribe file of a cantilever geometry for the membrane with only one foot

In the future optimal shooting parameters have to be found and other geometries for the membranes could be tested to further reduce cracks. For example the strain, that occurs through the shrinkage, would

be more homogeneously distributed with a round membrane model (see picture 6.1). Cracks, that are occurring due to the strain, could also be prevented by a cantilever geometry (see picture 6.2). For these models new working printing parameters would have to be found.
Moreover the developing process should be adjusted so, that no GP-Silica stains are left on the substrate. Then the coupling depth and the resulting Q-factor of the membranes made of GP-Silica could be compared to the coupling depths and the Q-factors of the other membranes made with the resin IP-S to see, if the Q-factor can be increased by using glass membranes.
If the printing and shooting parameters can be further optimised, the membranes out of glass would improve the Q-factor by several orders of magnitude. By adjusting the parameters and geometries additionally to get more strain in the membranes the Q-factor could be increased even more.

APPENDIX A

Appendix

A.1 Shooting parameters

Table A.1: shooting parameters of 4.5, y_{diff} = 5.284 mm

shot	pulse duration[ms]	number of pulses	laserpower[W]	delay[ms]
1	10	10	0.08	50
2	10	20	0.08	50
3	10	30	0.08	50
4	10	40	0.08	50
5	10	10	0.09	50
6	10	20	0.09	50
7	10	30	0.09	50
8	10	40	0.09	50
9	10	10	0.10	50
10	10	20	0.10	50
11	10	30	0.10	50
12	10	40	0.10	50
13	10	15	0.15	100
14	8	10	0.12	100
15	8	15	0.12	100
16	8	8	0.12	100
17	8	10	0.11	100
18	8	10	0.13	100
19	8	10	0.14	100
20	8	15	0.12	100

Table A.2: shooting parameters of 4.6, y_{diff} = 5.284 mm

cuboid	pulse duration[ms]	number of pulses	laserpower[W]	delay[ms]
1	10	10	0.12	80
2	10	20	0.12	80
3	10	30	0.12	80
4	10	40	0.12	80
5	10	50	0.12	80
6	8	10	0.15	80
7	8	15	0.15	80
8	8	20	0.15	80
9	8	25	0.15	80
10	8	30	0.15	80
11	8	10	0.12	100
12	8	20	0.12	100
13	8	20	0.10	100
14	8	30	0.10	100
15	8	40	0.10	100
16	8	1	0.15	100
17	8	2	0.14	100
18	8	3	0.14	100
19	8	4	0.14	100
20	8	5	0.14	100
21	10	5	0.10	100
22	10	6	0.10	100
23	10	7	0.10	100
24	10	8	0.10	100
25	10	9	0.10	100

Table A.3: shooting parameters of 5.4: pulse duration $\tau = 8\,\text{ms}$, delay between pulses $\tau_\Delta = 16\,\text{ms}$, $y_{diff} = 5.775\,\text{mm}$

membrane	number of pulses	pulse	AOM voltage [%]	laserpower P_0 [W]
1	10	1-2 3-8 9-10	50 100 50	0.20
2	15	1-3 4-12 13-15	50 100 50	0.20
3	20	1-4 5-16 17-20	50 100 50	0.20
4	20	1-4 5-16 17-20	50 100 50	0.25
5	15	1-3 4-12 13-15	50 100 50	0.25
6	10	1-2 3-8 9-10	50 100 50	0.25
7	10	1-6 7-8 9-10	100 50 25	0.23
8	15	1-9 10-12 13-15	100 50 25	0.23
9	20	1-12 13-16 17-20	100 50 25	0.23

A.2 Printing parameters

Table A.4: printing parameters of membranes that are shot on

membrane	LP [%]	ScSp [µm/s]	HD (feet) [µm]	SD (feet) [µm]	HD [µm]	SD [µm]
4.9	84	7500	0.08	0.18	0.04	0.15
4.10	90	7500	0.08	0.18	0.04	0.15
4.11	80	7000	0.08	0.18	0.04	0.15
4.12	85	7500	0.08	0.18	0.04	0.15
4.13	90	7500	0.08	0.18	0.04	0.15
4.16	90	7500	0.08	0.18	0.04	0.15
4.17	90	7500	0.08	0.18	0.04	0.15
4.22	90	7500	0.08	0.18	0.04	0.15

A.3 Recommended post thermal treatment of GP-Silica

'GP-Silica Standard' thermal processing program

hide

1. Debinding step

L9	move substrate lift all the way up
T8400.C90	heat the chamber to 90 °C in 8400 s
T10800	wait for 10800 s
T18000.C150	heat the chamber to 150 °C in 18000 s
T10800	wait for 10800 s
T24000.C230	heat the chamber to 230 °C in 24000 s
T10800	wait for 10800 s
T15000.C280	heat the chamber to 280 °C in 15000 s
T10800	wait for 10800 s
T48000.C600	heat the chamber to 600 °C in 48000 s
T7200	wait for 60 s
/2	jump to program number 2, which is the sintering step in this example, as follows

2. Sintering step

L9	move substrate lift all the way up
V8	set vacuum level to 8 (150 mbar)
T60	wait for 60 s
V9	set vacuum level to 9 (<70 mbar)
T003.C1300	temperature ramp which increases the temperature in the chamber to 1300 °C in steps of 3 °C per minute
T7200	wait for 7200 s
/3	jump to program number 3, which is the cooling step in this example, as follows

3. Cooling step

C0	turn off heating
V0	turn off vacuum (ambient pressure)
T003.A100	temperature ramp which decreases the temperature in the chamber to 100 °C in steps of 3 °C per minute
C0	turn off heating
T7200	Wait for 7200 s
L9	move substrate lift all the way up to leave the oven closed avoiding moisture entering the process chamber

Figure A.1: GP-Silica standard thermal processing program [11]

'GP-Silica Fast' thermal processing program

hide

1. Debinding and sintering step

L9	move substrate lift all the way up
V8	set vacuum level to 8 (150 mbar)
T60	wait for 60 s
V9	set vacuum level to 9 (<70 mbar)
T003.C1300	temperature ramp which increases the temperature in the chamber to 1300 °C in steps of 3 °C per minute
T7200	wait for 60 s
/7	jump to program number 7, which is the cooling step in this example, as follows

2. Cooling step

C0	turn off heating
V0	turn off vacuum (ambient pressure)
T003.A100	temperature ramp which decreases the temperature in the chamber to 100 °C in steps of 3 °C per minute
C0	turn off heating
T7200	wait for 7200 s
L9	move lift all the way up to leave the oven closed avoiding moisture entering the process chamber

Figure A.2: GP-Silica fast thermal processing program [11]

Bibliography

[1] C. M. Caves, *Quantum-Mechanical Radiation-Pressure Fluctuations in an Interferometer*, Phys. Rev. Lett. **45** (1980) 75, URL: https://doi.org/10.1103/PhysRevLett.45.75 (cit. on p. 1).

[2] J. Clarke, P. Neveu, K. Khosla, E. Verhagen and M. Vanner, *Cavity quantum optomechanical nonlinearities and position measurement beyond the breakdown of the linearized approximation*, Phys. Rev. Lett. **131** (2023), URL: https://doi.org/10.1103/PhysRevLett.131.053601 (cit. on p. 1).

[3] J. Thompson et al., *Strong dispersive coupling of a high-finesse cavity to a micromechanical membrane*, nature **452** (2008) 72, URL: https://doi.org/10.1038/nature06715 (cit. on p. 1).

[4] L. Tenbrake, A. Faßbender, S. Hofferberth, S. Linden and H. Pfeifer, *Direct laser-written optomechanical membranes in fiber Fabry-Perot cavities*, Nature Communications **15** (2024), URL: https://doi.org/10.1038/s41467-023-44490-7 (cit. on p. 1).

[5] Nanoscribe, *Laser*, URL: https://support.nanoscribe.com/hc/en-gb/articles/360010926139-Laser (visited on 04/01/2025) (cit. on p. 1).

[6] Nanoscribe, *Polymerization Mechanism of IP-Resins*, URL: https://support.nanoscribe.com/hc/en-gb/articles/360011291214-Polymerization-Mechanism-of-IP-Resins (visited on 04/01/2025) (cit. on p. 1).

[7] Nanoscribe, *3D Printing using Two Photon Polymerization (2PP)*, URL: https://support.nanoscribe.com/hc/en-gb/articles/360008908273-3D-Printing-using-Two-Photon-Polymerization-2PP (visited on 04/01/2025) (cit. on p. 1).

[8] Nanoscribe, *Galvo*, URL: https://support.nanoscribe.com/hc/en-gb/articles/360010850700-Galvo (visited on 04/01/2025) (cit. on pp. 1, 4).

[9] D. Stachanow, *Manufacturing Q-optimized polymer-based mechanical resonators for cavity optomechanics with 3D direct laser writing, master thesis*, 2024 (cit. on pp. 1, 30, 31).

[10] J. Lin et al., *Femtosecond laser direct writing of high-Q microresonators in glass and crystals*, Proceedings of SPIE - The International Society for Optical Engineering **9343** (2015), URL: https://doi.org/10.1117/12.2071737 (cit. on p. 1).

[11] Nanoscribe, *Printing with the Glass Printing Explorer Set (GP-Silica)*, URL: https://support.nanoscribe.com/hc/en-gb/articles/4402084033810-Printing-with-the-Glass-Printing-Explorer-Set-GP-Silica (visited on 02/01/2025) (cit. on pp. 2, 4–6, 9, 16, 39, 40).

[12] Nanoscribe, *GP-Silica*, URL: https://support.nanoscribe.com/hc/en-gb/articles/360022237999-GP-Silica (visited on 02/01/2025) (cit. on pp. 3, 4).

[13] Nanoscribe, *63x Objective*, URL: https://support.nanoscribe.com/hc/en-gb/articles/360002471754-63x-Objective (visited on 04/01/2025) (cit. on pp. 4, 7, 10).

[14] Nanoscribe, *ITO-Coated Substrates (3D MF DiLL)*, URL: https://support.nanoscribe.com/hc/en-gb/articles/360001695714-ITO-Coated-Substrates-3D-MF-DiLL (visited on 04/01/2025) (cit. on p. 4).

[15] Nanoscribe, *Cleaning Objective Lenses*, URL: https://support.nanoscribe.com/hc/en-gb/articles/360001457353-Cleaning-Objective-Lenses (visited on 02/01/2025) (cit. on p. 5).

[16] Henry-Schein, *DEKEMA AUSTROMAT® 674*, URL: https://www.henryschein.com/us-en/zahn/DigitalDentistry/dekema-austromat-674.aspx (visited on 19/01/2025) (cit. on p. 5).

[17] M. Scharfstädt, *Implementation of a micro-mirror production setup for information applications, master thesis*, 2022 (cit. on pp. 17, 18, 20).

[18] L. Tenbrake, *Fiber Cavity Optomechanics with Polymer Membranes, master thesis*, 2021 (cit. on pp. 19, 29–31).

[19] L. Lévesque, *Law of cooling, heat conduction and Stefan-Boltzmann radiation laws fitted to experimental data for bones irradiated by CO_2 laser*, Biomedical Optics Express **5** (2014) 701, URL: https://doi.org/10.1364/BOE.5.000701 (cit. on p. 24).

[20] P. Tipler, G. Mosca, P. Kersten and J. Wagner, *Physik für Studierende der Naturwissenschaften und Technik, 8.Auflage*, 2008 (cit. on p. 24).

[21] LEIFIphysik, *Dichten verschiedener Stoffe*, URL: https://www.leifiphysik.de/mechanik/masse-volumen-und-dichte/ausblick/dichten-verschiedener-stoffe (visited on 20/01/2025) (cit. on p. 24).

[22] F. Giefer, *Towards a Double Tip Vacuum Fiber Microscope, bachelor thesis*, 2022 (cit. on p. 30).